Interactive comment on "Impact of mineral dust on shortwave and longwave radiation: evaluation of different vertically-resolved parameterizations in 1-D radiative transfer computations" by Maria José Granados-Muñoz et al

Anonymous Referee #1

We would like to thank the reviewers for their efforts and thorough review of our manuscript. We realize that the notes and suggestions made will improve the quality of the paper. Hereafter, the reviewers' comments are presented in bold font and the text included in the manuscript is marked in italics. Line numbering is referred to the new version of the manuscript.

The paper presents an analysis of the optical and microphysical properties of dust particles observed from ground and from airplane on 16-17 June 2013 above southeastern Spain during the ChArMEx/ADRIMED campaign. The observations were conducted during a moderate Saharan dust event. Using a 1-D radiative transfer model, the author makes comparison of the output results obtained with different input data. They consider both shortwave and longwave radiation for the calculations. They concluded that the dust produces a cooling effect both at the surface and at the top of the atmosphere, as expected.
The paper in well written, the methodology and the results are clearly presented. The discrepancies coming from the different parametrizations are well analyzed. The authors conclude that global model estimate needs to consider the complete radiation spectrum to avoid an overestimation of the cooling effect produced by dust.
I have just one major concern. The same dust event was observed are almost the same location and at the same time by a balloon borne aerosol counter LOAC (Renard et al., Atmos. Chem. Phys., 18, 3677-3699, 2018, https://doi.org/10.5194/acp-18-3677-2018). Such counter measurements can be considered here for the estimate of the vertical distribution of the dust plume, and for the size distribution of the particles.

The ballon borne measurements included in Renard et al., (2018) were performed at the stations of Minorca and Ile du Levant. These locations are around 700 km away from Granada, therefore, no data are available at Granada station where the current study is performed.

The paper can be published if the comments below are considered.

1. **Abstract: A sentence must be added on the cooling effect found by the authors.**

Done.
Page 2, lines 6-7: *"The three parameterization datasets produce a cooling effect due to mineral dust both at the surface and the top of the atmosphere."*

2. Instrument and data: Perhaps a map of the ground-based and airplane locations could be added.

The map is already included in Benavent-Oltra et al., 2017 (Figure 1), as indicated in the manuscript (Page 6, line 24).

3. Page 8 line 25: Such observation were also reported by Renard et al. 2018.

The study by Renard et al. (2018) is included as a reference in the manuscript where appropriate.

4. Page 10 line 9: The authors say that the concertation profiles of the main absorbing gas were taken from the US standard atmosphere. Nevertheless, real profiles can exhibit a significant variably from the standards for several reasons (local event, perturbed atmosphere. . .). Can you evaluate the effect of this variability on your results?

Variations in the concentration of the main absorbing gases have a low impact on the radiative fluxes profiles and much lower impact in the ARF, since only the effect of the aerosol is accounted for. As an example, we performed a sensitivity test varying the ozone profiles up to double concentrations. Comparing the obtained results with those obtained for DS1 using the standard concentration, we observe differences lower than 4 $W \cdot m^{-2}$ in the $^{\downarrow}F_{SW}$ and lower than 2 $W \cdot m^{-2}$ in the case of the $^{\uparrow}F_{SW}$. For the LW, differences lower than 1.5 $W \cdot m^{-2}$ in the $^{\downarrow}F_{LW}$ and lower than 3.6 $W \cdot m^{-2}$ in the case of the $^{\uparrow}F_{LW}$ are obtained. For the ARF differences are negligible (below 0.2 $W \cdot m^{-2}$).

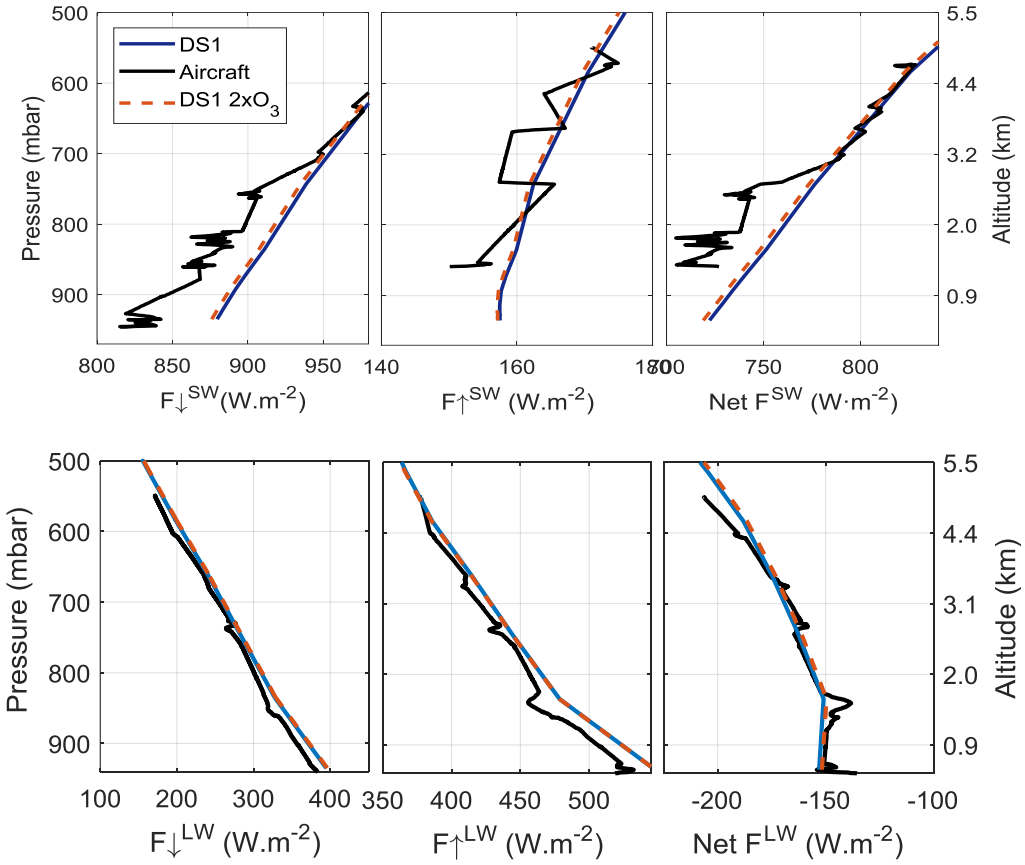

Figure. Radiative fluxes for the SW (top) and LW (bottom) spectral range for June 16 simulated with GAME using DS1 (in blue) and DS1 with double ozone concentration (orange dashed line). The black lines are the aircraft in situ measurements.

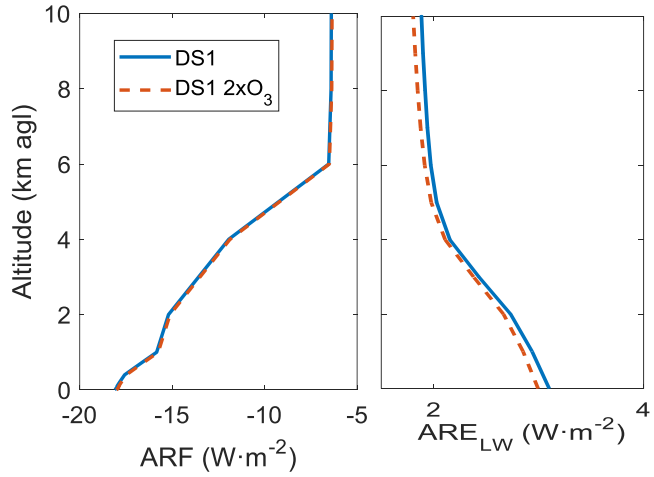

Figure. ARE profiles in the SW (right) and LW (left) spectral ranges simulated using DS1 (blue line) and DS1 with double ozone concentration (orange dashed line) as input data in GAME for June 16.

5. Page 10 line 15: The authors could consider the LOAC measurements, and the detection of large particles that produce a third mode.

We agree with the reviewer that the LOAC would provide very valuable information for our study. Nonetheless, no LOAC measurements are available above Granada site.

6. Page 13 line 10:
The author say that the refractive index of the dust are assumed to be constant with altitude. I understand that it is difficult to detect a possible variation of the index with altitude. Nevertheless, the authors must discuss the limit of this assumption, and how a variation of the refractive index can affect their results. They can consider the variability of the refractive index for different natures of dust and for the possible presence of pollution particles.

For our study we assumed the refractive index provided by Di Biagio et al., (2017) for the Moroccan source, which we consider as the most appropriate for our case studies. By using the refractive index provided for the Algerian and Mauritanian sources from the same database we observe variations in the ARF at the BOA of 0.8 $W \cdot m^{-2}$ and 0.3 $W \cdot m^{-2}$ at the TOA. These results come to confirm the importance of having an accurate aerosol database for the retrieval of the ARF and the reduction of the uncertainties. They have been reported in the new version of the manuscript:
Page 14, lines 20-25: *"This assumption is not exempt of uncertainty, since the refractive index present a certain variability associated to the different nature of mineral dust properties. For example, the use of the refractive index provided for the Algerian and Mauritanian sources from Di Biagio et al., (2017) leads to variations in the ARF of 0.8 and 0.3 $W \cdot m^{-2}$ at the BOA and the TOA respectively. Additionally, vertical variations of the refractive index are also a source of uncertainty in the obtained radiative fluxes."*

7. Page 13 line 12: Is it "interpolation" or "extrapolation"?

Text has been modified. Interpolation has been replaced by extrapolation.

8. Page 13 line 23: The authors must also consider the LOAC balloon borne aerosol counting data.

See our previous responses on this topic.

9. Page 17 line 26: Do you think that the presence of large dust particles, not always detected from aircraft instruments, could partly explain the large differences you observe?

We agree that the presence of large particles may partly explain the differences observed in the longwave radiative fluxes. As stated in the introduction, large particles are especially relevant for the aerosol radiative forcing in the longwave range. Therefore, it is important to consider the presence of these large particles in the aerosol measurements required to feed radiative transfer models. As an example, we performed a simulation with our model considering a third mode with similar characteristics to the one observed during this dust event in Minorca. On June 16, by adding this third mode (assuming that the number concentration is a 15% of the coarse mode) we observe an increase in the ARF_{LW} of 0.5$W \cdot m^{-2}$ at the BOA and 0.25 $W \cdot m^{-2}$ at the TOA. This increase in the ARE due to the presence of a third mode is significant, but it does not fully explain the differences observed here.

Interactive comment on "Impact of mineral dust on shortwave and longwave radiation: evaluation of different vertically-resolved parameterizations in 1-D radiative transfer computations" by Maria José Granados-Muñoz et al Anonymous Referee #2

We would like to thank the reviewers for their efforts and thorough review of our manuscript. We realize that the notes and suggestions made will improve the quality of the paper. Hereafter, the reviewers' comments are presented in bold font and the text included in the manuscript is marked in italics. Line numbering is referred to the new version of the manuscript.

This work focuses on analyzing the differences in the aerosol radiative forcing obtained by the same radiative transfer model (GAME) using different datasets as input, during a dust intrusion in the Iberian Peninsula within the ADRIMED/CHARMEX campaign. The methodology that the authors use in this work is sound, and similar research has been already done in previous papers in order to analyze the sensitivities of radiative fluxes and aerosol radiative forcing (e.g. Gómez-Amo et al., 2010; 2011; Meloni et al. 2015; 2018), and aerosol heating rates (e.g. Meloni et al. 2015; Peris-Ferrús et al., 2017), to the aerosol properties used as input in the radiative transfer models. Despite this, the most novel and interesting part of this work is the comparison between the results obtained using a very advanced and complete characterization of the aerosol properties, as well as their vertical distribution (GRASP) against those obtained from most known and widely used measurements and algorithms (i.e. Klett inversion lidar + photometer; and airborne in situ measurements). This reason is sufficient for this paper to be
of interest for aerosol research in order to understand the uncertainties associated to aerosol radiative effect. Therefore, the argument of this paper is solid and then suitable for publication in ACP. However, I think there are several important aspects that can be improved, and it should be addressed before the paper is published.

GENERAL ASPECTS
In general, I miss a deeper analysis of the results, especially from a quantitative point of view.
1. Therefore, I would suggest that the authors focus their work on estimating the sensitivity of the GAME model to the different aerosol inputs., answering the following question that underlies their own figures: why the authors observe notable differences in the ARE among the datasets, in shortwave and longwave ranges, despite the differences in the vertical profiles of radiative fluxes they obtain are negligibles?. This should be done in a quantitative way by taken into account the differences among the aerosol properties used in the three datasets.
2. For this, I think that the differences among the aerosol datasets used should be better explained, in terms of the aerosol properties (i.e. extinction, absorption and scattering): If I understand well the inputs that GAME model requires for aerosol characterization ext(wavelength,z), SSA(wavelength,z) and asymmetry parameter(wavelength,z):
a. In the shortwave range DS1 - GRASP provides the spectral profiles (7 wavelengths) of the aerosol extinction and SSA. DS2 - However, the Klett inversion only provides the spectral (3 wavelengths) extinction profile (taking into account vertically constant LR). The SSA is constant with height and column-integrated AERONET values (4 wave-lengths) are assumed. DS3 - Airborne measurements also provide information about extinction and absorption profiles; with no spectral considerations. In the three cases the column-integrated AERONET asymmetry parameter (4 wavelengths) is assumed. This information is well summarized in Table 2, but I miss better explanation in the text.

The differences in ARE observed between the three datasets are comparable to those observed in the radiative fluxes in absolute terms and therefore the results are consistent. A thorough quantitative discussion on the differences between the aerosol properties was already presented in Benavent-Oltra et al. (2017) and thus it was out of the scope of the present study. However, additional information has been added to the manuscript for completeness considering the reviewer's suggestion. Additionally, a small paragraph summarizing Table 2 and Section 3.2.2 has been added.
Page 14, lines 1-8: *"Summing up, for the SW aerosol parametrization in GAME three datasets are tested. In DS1, GRASP provided spectral profiles at 7 wavelengths of the aerosol extinction and SSA are used. In*

DS2, the Klett retrieved extinction profiles at 3 wavelengths are used together with the AERONET SSA columnar values at 4 wavelengths, which are assumed to be constant with height. For DS3, one extinction profile at 550 nm and a column-averaged single-wavelength value of the SSA from the airborne measurements are considered. In the three cases, the column-integrated AERONET asymmetry parameter at 4 wavelengths is assumed to be constant with height and used as input."

On the other hand, there is a different aerosol layering among the studied days that can play an important role on the retrieved ARE. Looking at the aerosol extinction profile (Figure 2) and the concentration of Fine and Coarse modes (Fig. 5): June 16, a single homogeneous aerosol layer is observed June 17, aerosol are uncoupled in two layers. The same is observed in the SSA profiles shown in Fig. 3. have you consider to analize the role of aerosol layering in your retrieval?

We thank the reviewer for this suggestion. Because of the different SZA during both days and the different atmospheric conditions, a direct comparison between June 16 and 17 in order to study the influence of the aerosol layering is not possible. However, additional comments on the aerosol layering influence on the ARE are now included in the text considering the information available in the literature (e.g. Meloni et al., 2004; Guan et al., 2010). These studies show that the vertical structure of the aerosol has lower impact in the ARF at the surface level for low-to-moderate absorbing particles, which should be our case for mineral dust.

b. In the longwave range. The authors obtain the aerosol properties by Mie calculations as appears in Tables 2 and 4. However, it is not clear what radius are used in Mie calculations. Sometimes the authors assert they use the reff and nevertheless, in table 4 the radii appear in the 2 modes (fine and coarse). Please be clear and consistent.

The radii values presented in Table 4 are those corresponding to the effective radius of both the fine and the coarse modes. We show these values here because they are directly taken from the different databases. These data are later on processed and converted to the corresponding modal median radius for Mie calculations. Text and corresponding symbols have been modified for clarity purposes.

3. The results should be analized taking into account the quantitative differences among the aerosol properties used in the aerosol datasets, considering - spectral variation- vertical variation. Considering that the main differences among the aerosol datasets are based on differences in the vertical profile of extinction and absorption, the authors should take into account the work already published in this regard, using other models and different datasets. For example, to help in the interpretation of the differences observed in the shortwave, I would recommend reading of: Meloni et al. 2005. Where the effect of the extinction profile on the calculation of the ARE is analyzed. Different works by Gómez-Amo et al., 2010 and 2011, as well as by Guan et al., 2010. Where the effect of vertically varying the aerosol absorption in the determination of ARE is analyzed.

We thank the reviewer for these references. Additional discussion considering the results presented by those authors is now included in the manuscript (e.g. Page 17, lines 3-5: *"The vertical distribution of the SSA also influences the radiative fluxes in the SW as demonstrated in previous studies (Gomez-Amo et al., 2010; Guan et al., 2010), contributing to explain the differences observed among the three datasets analyzed here."*)

Main concerns about results and conclusions sections: SW: Is difficult to understand that with such small differences among the different dataset input (below 1% for radiative fluxes and 0.05 for AOD), why do the authors obtain such large differences in the AREsw (up to 33%)? I think that this is the question you have to answer in this paper, using your data and simulations, which is missing in this paper. At fixed solar zenith angle, the shortwave fluxes are mainly dependent on the AOD. The direct flux is totally driven by the extinction (AOD) and with such small AOD variations between datasets I do not expect large differences in the fluxes (just what you obtain and is shown in Fig. 5 and 6). However, the diffuse radiation is extremely dependent on SSA and the phase function (i.e. asymmetry

parameter). If AOD and asymmetry parameter remain fixed, Gómez-Amo et al., (2010) showed that the differences observed in the ARF (at the surface and TOA) are driven by the vertical distribution of SSA that results in different distribution of the diffuse radiation. I would suggest repeating the analysis by removing the small variation of AOD. For example by normalizing the three datasets to the AERONET AOD, or working with the forcing efficiency, and focus the analysis on the variations due to the SSA.

The AOD difference on June 16 is 0.05, which represents nearly a 22% variation with respect to the AERONET AOD, and therefore is small but still significant, leading to corresponding differences in the ARE. Besides, we have performed a sensitivity study by fixing all the parameters except one as suggested by the reviewer to analyze the influence of each parameter on the final results and we have included the forcing efficiency values. Additional discussion is now included in the manuscript according to these results where appropriate. As for the ARE differences, if we understand the reviewer's point, even though they are large in relative values, absolute values are below 15 $W \cdot m^{-2}$, which is in the same range of the differences obtained for the fluxes. According to the ARE definition, the differences in the ARE obtained values are coherent with the differences in the fluxes.

I think it would be useful for the interpretation of the results: - to show in Fig. 4 the spectral variation of SSA for the 2 layers observed on June 17, and for the homogenous layer on June 16. - the vertical profiles of SW and LW fluxes in aerosol-free conditions should be shown in Fig. 6 and 9., respectively. (see Meloni et al., 2015; 2018)

Unfortunately, spectral variation of the SSA is not provided by the aircraft measurements and it is not possible to include it in Fig. 4 for the different layers. The more complete information regarding the vertical distribution of the SSA is already provided by GRASP results in Fig. 3. The aerosol-free conditions profiles are now included in Figs. 6 and 9.

LW: P20-L20: I do not understand this sentence: "Considering the low influence of the aerosol in the LW radiative fluxes, the influence of the assumed CO2, O3 and the used water vapor profiles and LST are needed to fully explain this discrepancy". Why do you think that the differences in the LW fluxes are due to the assumed CO2, O3 and the used water vapor profiles and LST? Did you change them among the simulations DS1, DS2 and DS3? According to table 4, these values do not change with the dataset considered.

The reviewer is right, these values did not change for the simulations using DS1, DS2 and DS3. We mean here the differences between GAME retrievals and the aircraft data. The sentence has been modified to make it more clear.

Page 22, lines 21-23: **"***Considering the low influence of the aerosol in the LW radiative fluxes, the influence of the assumed CO_2, O_3 and the used water vapor profiles and LST are needed to fully explain this discrepancy between the aircraft and the simulated profiles.***"**

Fig 12. The authors report an ARE offset LW/SW increase with altitude, up 90% at higher altitudes, when there was not aerosol layer anymore. This is totally opposite at what is reported in Meloni et al., (2015), that found the maximum offset at the surface and a negligible variation from the top of the aerosol layer to the TOA. These results should be better discussed and justified.

A few nuances with regard to the reviewer's comment are necessary to answer this point; there are some similarities between our work and Meloni et al. (2015) but also some differences that need to be considered.

1. We also find that the LW/SW ratio between the highest aerosol layer and the TOA is nearly constant (see Figure 12).
2. In Meloni et al. (2015), SZA = 55.1º. This is comparable to our results on June 17, when SZA = 61.9º. If we look at the evolution of the LW/SW ratio between the surface and the highest aerosol

layer (~4 km) on that day a decrease is observed for all datasets (the highest decrease is ~40% for DS3). This decrease in Meloni et al. (2015) is ~50 %.

3. The behavior of the LW/SW ratio plots above the highest aerosol layer may have some intrinsic artefacts due to the different vertical resolutions of the SW and LW model versions. As can be seen in Table 1, the SW version has a 2-km resolution between 2 and 10 km and the LW version has a 1-km resolution below 25 km. This makes that the vertical distribution of the AOD per layer (in the parametrization of GAME) near the top of the aerosol layer is different between both SW and LW spectral ranges. If we take DS3 on 16 and 17 June, the ARE_{SW} slightly decreases between 6 and 8 km (Fig. 8) while the LW ARE_{LW} is constant above 6 km (Fig. 11). This effect will produce an artificial increase of the LW/SW ratio near or just above the top of the dust layer, which may not be necessarily insignificant as shown on the profile of DS3 on Fig. 12a.

Minor comments:

P2-L3: Please change "contrasted" by "compared" Done.

P2-L21: Please rephrase the sentence, its meaning is no clear. Done.

P4-L5: Please change "..model estimates sensitivity..." by "..sensitivity of the model estimates.." Done.

P5-L2: Please change "..real and imaginary refractive indices..." by "..real and imaginary parts of the refractive index.." Done.

P5-L24:Plase remove "particle" Done.

P5-L29: Please change "..spatial integral..." by "..vertical integration.." Done.

P6-L6: Please change "in" by "by" Done.

P9-L27: How the surface temperature was estimated from the measurements at 2m above the ground? please provide a reference. Done.

The LST is assumed to the temperature measured at the meteorological station, located at 2 m agl. The sentence has been rephrased and discussion is now added regarding this assumption.

Page 19, from line 25: *"On this latter day, larger differences are observed on the Net F_{LW} compared to 16 June, which might be explained by the inaccurate value of LST used due to the lack of precise data. A sensitivity test performed by increasing the air surface temperature measured at the meteorological station 5K indicates that the $^{\uparrow}F_{LW}$ increases its value up to 30 $W{\cdot}m^{-2}$ at the surface, and around 10 $W{\cdot}m^{-2}$ from 1 km onwards which is non-negligible. This would lead to an overestimation of the aircraft measured values, but still within a 6% difference. This highlights the need for accurate LST measurements for radiation simulations in the LW spectral range."*

P11-L12: This sentence is really surprising. I do not understand well the differences in the AOD among the datasets reported in table 4. Since the AOD measured with the CIMEL photometer is imposed as a closure condition in the GRASP and Klett inversions, one would expect similar AOD for DS1 and DS2 datasets, contrarily to what is reported in Table 4. On the other hand, AOD differences are expected from DS1 and DS2, with respect to DS3 (aircraft exctinction). These differences may be also due to the AOD content from surface to the minimun altitude of the aircraft, or for the observation of different airmasess (20km far from ground-based station and aircraft). I think the authors should clearly discuss these AOD differences, since the discussion about the differences in the ARE results is mainly addressed in terms of AOD.

In our case, the AOD indicated in Table 4 is not exactly the one provided by GRASP, but the integral of the extinction profiles between the surface and the altitude assumed in this work as the top of the aerosol layer, which are the ones used as input for GAME simulations. The GRASP extinction values above this assumed top layer are not null since GRASP assumes stratospheric aerosol presence which exponentially decreases with altitude from the highest altitude used as input (as can be seen in Lopatin et al. (2013), being the GARRLiC scheme the same used in GRASP lidar retrieval). This fact makes that the integrated GRASP extinction used in this work (integrated until the assumed top aerosol layer but not until TOA) underestimates the AOD from AERONET (stratospheric aerosol is not considered). For the comparison

presented here we consider it is more accurate to consider only the region between the surface and the assumed top of the aerosol layer so that we have homogenous criteria for the three datasets. Thus, a larger difference than the uncertainty is obtained between DS1 and DS2.
Page 11, line 24 – Page 12, line 6: *"The AOD values presented here (included in Table 4) are obtained by integrating the α_{aer} profiles at 550 nm from the surface up to the considered top of the aerosol layer (4.3 km on June 16 and 4.7 km on June 17). In GRASP retrieved α_{aer} profiles, values above this top of the aerosol layer are slightly larger than zero since GRASP takes into account stratospheric aerosols by an exponential decay (Lopatin et al., 2013), thus the approach used here to calculate the AOD leads to lower values compared to the column-integrated AOD provided by the sun-photometer. Differences among the three datasets are more noticeable on June 16, when the AOD for DS1 is 0.05 lower than for DS2 and DS3, whereas on June 17 the maximum difference is 0.03, obtained between DS1 and DS2."*

P13-L2: This approach is similar to the used in Meloni et al., (2015,2018) and Peris-Ferrús et al., (2017). This papers should be cited in this paragraph.

References have been added.

P13-L11: Are you sure about this sentence? Is there any typo error? wavelengths below 3 um are not considered LW range. What about for wavelengths over 16 um?

The Mie code in GAME requires this info to perform the computations of the aerosol properties in the LW. Extrapolation for longer wavelengths is also used, text has been corrected.

P13-L14: What radius did you use in Mie calculations? the effective radius, or the rF and rC? Table 4, Table 4 caption and the text result confusing. Please be clear.

See previous response.

P14-L11. Please change "visible" by "shortwave" Done

P14-L12. Please change "thermal" by "longwave" Done

P14-L27. When the authors talk about "discrepancies", are they refeering to "relative differences" (Fgame- Faircraft)/Faircraft? The authors should define how they obtain these discrepances, and always use the same term. Sometimes they use "discrepancies" and sometimes"differences".

Discrepancies here is referred to the absolute difference between the simulated fluxes obtained by the three datasets. Text has been reviewed according to the reviewer's comment to account for possible inconsistencies. The difference with the aircraft data is not considered in this part or the manuscript. In case of relative differences, it is now explicitly indicated in the text and it is defined how they are calculated.

P15-L5. Please clarify the meaning of this last sentence of the paragraph. The main aerosol effect over the radiative fluxes is due to the AOD, the SSA is a second order effect.

We agree with the reviewer that this sentence was confusing. It has been rephrased.
Page 16, line 26- Page 17, line 2: *"In our case, the larger AOD assumed for DS2 on both days (see Table 4 and Figure 2), causes the ↓FSW to be slightly lower compared to DS1. For DS3 the AOD is similar to DS2, but the SSA values used, which are relatively smaller compared to those measured by AERONET (see Figure 4), lead to lower values of the radiative fluxes than for DS2."*

P15-L11. I do not see the influence of the boundary layer due to the distance between the ground-based station and the aircraft leg. The DS3 simulation is set with the aircraft data, so the 20 km distance between the ground-based station and the aircraft leg should be reflected in the results obtained from the DS3 simulation.

Removed

P15-L17. The authors should take into account that relative differences about 7% for a Fdownward around 430 and 530 Wmˆ-2 yield absolute differences of 30 and 37 Wmˆ-2. These differences may represent a large fraction of the aerosol effect, with a large contribution to the uncertainties in the determination of ARE using this data. I don't think that these differences are quite insignificat as the authors assert. Have you evaluated them?

The 7% value indicated in the manuscript correspond to the maximum difference observed, whereas on average differences are below 4%. Considering that the maximum difference observed between the three datasets reaches 19 $W \cdot m^{-2}$ and the uncertainty of the pyranometer is 5 $W \cdot m^{-2,}$ together with the differences between the aircraft and the model in vertical resolution, time sampling and data acquisition and processing techniques a difference of 30 $W \cdot m^{-2}$ between GAME and the aircraft measurements is quite reasonable. Additionally, the uncertainties introduced due to the use of the standard atmosphere or the parameterization of the surface properties may also be partly responsible of the differences observed here. When calculating the ARE, the uncertainties due to the vertical resolution of the model, temporal sampling and the assumption of the standard atmosphere, the gases concentration or surface parameters are minimized.

P15-L27. Again, a 60 Wmˆ-2 differences between datasets may contribute to large uncertainties in the determination of ARE using this data. Please evaluate this.

In order to understand the differences observed here an evaluation of the CM11 pyranometer data at the surface against AERONET $^{\downarrow}F_{SW}$ has been performed using the simultaneous data available on June 16 and 17 (6 pairs of data). AERONET surface radiative fluxes have been extensively validated at several different sites around the world by Garcia et al. (2008). In addition, all AERONET sun-photometers are mandatorily calibrated once a year. Large differences are obtained between AERONET and the CM11 pyranometer, reaching up to 130 $W \cdot m^{-2}$ in one of the cases. These results point out to a likely malfunction of the pyranometer during the campaign that would explain the differences observed. We have performed simulations with GAME for the time of the closest AERONET measurement on June 16 (at 16:22UTC), assuming that the aerosol parameterization is constant with time between the flight time and the photometer measurement (even though there is an AOD increase from 0.23 to 0.25 between 14:30 and 16:22UTC according to the sun-photometer data). This simulation provides $^{\downarrow}F_{SW}$ values at the surface of 564.8, 551.8 and 547.0 $W \cdot m^{-2}$, similar to the 531.4 $W \cdot m^{-2}$ provided by AERONET. On June 17, GAME simulations at 07:40UTC (instead of 07:30UTC, which is the time of the flight), provide values $^{\downarrow}F_{SW}$ at the surface of 466.3, 468.3 and 456.4 $W \cdot m^{-2}$, very close to the AERONET value of 463.7 $W \cdot m^{-2}$.

P16-L14. I think that the comparison GAME-CERES have no sense, even qualitatively, with CERES overpass 600km. The upward flux at TOA is mainly dependent on surface albedo and clouds, and both can be really different at 600km away. I would suggest remove this comparisons, since they do not present a relevant contribution to this work.

Removed

P17-L8:L15. Since this paper is mostly to analyze differences in ARE using different datasets. The authors should carry out a more in deep analysis of the results. Specially regarding to the surface and TOA values. Even if the values obtained for the three datasets fall within the range of the values previosuly observed in the Mediterranean, notice that the values shown in Table 6 differ from a 30-50%. These differences are really large and dependent on the used dataset, and consequently it should be analyzed in detail. Please take into account the following references to help with the interpretation.

Discussion has been extended taking into account the references suggested by the reviewer.

P17-L21. Please change "..from Mie calculations from..." by "..from Mie calculations for.."

Done.

P17-L23:P18-L4. I think that a more detailed analysis is needed to establish why you observe these differences between GAME and aircraft measurements. On 16 June, the differences may be explained "by the assumed profiles of gases such as CO2, O3 or water vapor, or the uncertainty in the LST", as the authors assert, or may be not. It is just a too simple qualitative explanation.

For the LW spectral range, the differences are mostly lower than 10 $W \cdot m^{-2}$, which can be considered within the uncertainty limits. Considering the uncertainty of the pyrgeometer, which is 5 $W \cdot m^{-2}$ and the fact that the aircraft and the model present different vertical resolutions and time samplings and the uncertainties due to the use of the standard atmosphere or the parameterization of the surface properties the obtained differences are not significant.

P18-L7. Please change "the diffuse radiation..." by " the longwave radiation.."

Done.

P18-L9. The differences observed are within the uncertainties of the pirgeometers, that for a well mantained and calibrated instrument are below 5 Wmˆ-2 (Meloni et al., 2012). Therefore, the authors does not need qualitative explanations based on variables as LST to justify the differences.
Removed.

P18-L11. As in the SW case, I think it is not worth including the comparison with CERES due to the large distance between the ground-based and satellite measurements.

Removed.

P18-L28. Please be consitent, rc or reffc?
We have updated all the symbols, using $r_{eff,c}$ and $r_{eff,f}$ for clarity.

Tables 6, 7, 8: The standard deviation is an statistical parameter then it have not sense if obtained over three values only.

It is included just as an indicator of the variability of the ARF values even though the number of simulations is low, as pointed out by the reviewer.

REFERENCES:

- Meloni, D., A. di Sarra, T. Di Iorio, G. Fiocco, Influence of the vertical profile of Saharan dust on the visible direct radiative forcing, Journal of Quantitative Spectroscopy & Radiative Transfer 93 (2005) 397–413

- Meloni, D., Di Biagio, C., di Sarra, A., Monteleone, F., Pace, G., and Sferlazzo, D. M.: Accounting for the solar radiation influence on downward longwave irradiance measurements by pyrgeometers, J. Atmos. Ocean. Technol., 29, 1629–1643, 2012.

- Gómez-Amo, J.L., A.diSarra, D.Meloni, M.Cacciani, M.P.Utrillas, Sensitivity of shortwave radiative fluxes to the vertical distribution of aerosol single scattering albedo in the presence of a desert dust layer, Atmospheric Environment 44 (2010) 2787-2791.

- Gómez-Amo, J.L., V. Pinti, T. Di Iorio, A. di Sarra, D. Meloni, S. Becagli, V. Bellantone, M. Cacciani, D. Fuà, M.R. Perrone, The June 2007 Saharan dust event in the central Mediterranean: Observations and radiative effects in marine, urban, and sub-urban environments, Atmospheric Environment 45 (2011) 5385-5393

- Peris-Ferrús, C., J.L. Gomez-Amo, C. Marcos, M.D. Freile-Aranda, M.P. Utrillas, J.A. Martínez-Lozano, Heating rate profiles and radiative forcing due to a dust storm in the Western Mediterranean using satellite observations, Atmospheric Environment 160 (2017) 142-153.

- Guan, H., B. Schmid, A. Bucholtz, and R. Bergstrom, Sensitivity of shortwave radiative flux density, forcing, and heating rate to the aerosol vertical profile, JOURNAL OF GEOPHYSICAL RESEARCH, VOL.115, D06209, doi:10.1029/2009JD012907, 2010

Interactive comment on "Impact of mineral dust on shortwave and longwave radiation: evaluation of different vertically-resolved parameterizations in 1-D radiative transfer computations" by Maria José Granados-Muñoz et al
Anonymous Referee #3

We would like to thank the reviewers for their efforts and thorough review of our manuscript. We realize that the notes and suggestions made will improve the quality of the paper. Hereafter, the reviewers' comments are presented in bold font and the text included in the manuscript is marked in italics. Line numbering is referred to the new version of the manuscript.

The paper examines a case of a moderate dust intrusion in Granada with the aim of calculating the dust radiative effect either in the SW and in the LW regions at the surface, at the top of the atmosphere, and within the dust layer by means of the GAME radiative transfer model. The focus of the study is the sensitivity of the SW and LW radiative fluxes and effects on the dust microphysical and optical properties derived in three different ways, using a combination of remote sensing (AERONET and lidar) measurements and the GRASP inversion code, and in situ airborne measurements from the SAFIRE ATR42 aircraft. This study is carried out in the framework of the ChArMEx/ADRIMED campaign and takes advantage of the large observation efforts placed during the project, using either ground-based, airborne and satellite observations. The results of the model calculations are those expected (SW cooling and LW heating by dust, with a not negligible LW/SW ratio), and the case study is not that of an extraordinary dust transport (AOD moderately low). However, the most important conclusion provided by the authors is that optical properties derived from different measurements and with different techniques may provide non-negligible differences in the radiative effects, and should be of concern when estimating dust forcing. I recommend publication, but after some major issues are resolved by the authors.

Major issues
The main issue on the presented results concerns the simulation of the SW irradiances using the three different aerosol optical properties DS1, DS2, and DS3, and the evaluation of the ARE. The authors found that very close SW irradiances at surface are obtained with the three datasets (the values seem coincident in Figure 7, but no quantitative information is provided in the text), while differences in the vertical profiles of the downward SW irradiances simulated with GAME are visible in Figure 6 close to the surface when using DS1 or DS2 (which seems to provide identical irradiances than DS3). So there seems to be an inconsistency between the simulations of the vertical profiles and of the surface SW irradiance.

The same values are represented in both Figures 6 and 7 for the different datasets. They seem inconsistent because of the scales and symbols used. Figures have been modified for clarity. Additionally, quantitative information about Figure 7 is now included in the text.

As a second point, the LW ARE is very low, due to the values of the AOD, and they might be comparable to the model uncertainties. So a careful evaluation of the uncertainties on the model output should be performed. The fact that the net LW irradiance on 17 June is overestimated by the model is likely not a problem of the CO2 and O3 profiles (the water vapor one should have been taken into account in the simulation, as it measured during the flights) used in the model (to my knowledge the impact of this minor gas is negligible), but comes from the fact that NET=Fâ ¿E ¸S-Fâ ¿ES, and Fâ ¿E ¸S is overestimated, while Fâ ¿ES is comparable to measurements. The model overestimation of the LW irradiance at the surface on 17 June (which, however, is as large as the measurement uncertainty) cannot be due to clouds affecting the measurements and not accounted in the model, because clouds increase the LW irradiance, and this should cause a model underestimation. I suggest to perform a sensitivity study to assess the uncertainty on the modelled SW and LW irradiances due to the uncertainty of the input parameters.

We agree with the reviewer that the uncertainty of the modelled irradiances should be estimated. However, a thorough evaluation of the uncertainty in GAME is out of the scope of the present study and it is worthy a publication itself. Anyway, we performed some sensitivity test to study the influence of the input parameters in the outcome of the model.
Variations of the SSA within the uncertainty values considered in AERONET (0.02-0.07 depending on the AOD) show a linear variation of the ARF_{SW} at the BOA reaching up to 10 $W \cdot m^{-2}$ for variations in the SSA of 0.07. In the case of the asymmetry parameter, a variation of 5% which is the uncertainty considered for AERONET data, changes of up to 2 $W \cdot m^{-2}$ are observed in the ARF at the BOA. In the case of the AOD, we observed a maximum variation in the F_{SW} of 6.5 $W \cdot m^{-2}$ (0.7%) at the surface, decreasing with height, for changes in the AOD of up to 0.05, which is the difference we observe between the AOD for DS2 and DS1 on June 16. Considering these results, the total uncertainty associated to the aerosol parameterization is approximately 12 $W \cdot m^{-2}$.

Page 16, line 17 onwards: "*In order to quantify these differences, we performed a sensitivity test by varying the AOD while the other parameters were kept constant. We observed a maximum variation in the F_{SW} of 6.5 $W \cdot m^{-2}$ (0.7%) at the surface, decreasing with height, for changes in the AOD of up to 0.05, which is the difference we observe between the AOD for DS2 and DS1 on June 16. This result partly explains the differences among the three datasets. In addition, a sensitivity test performed by varying exclusively the SSA indicates that more absorbing particles are related to less $^{\downarrow}F_{SW}$ at the surface, namely a variation of 1% is observed at the BOA for a decrease in the SSA of 0.03. The influence of the SSA decreases with height being negligible at the TOA. For the $^{\uparrow}F_{SW}$, a decrease of 0.8% is observed at the BOA if more absorbing particles are present, but in this case the influence at the TOA is larger (2.2%).*"

For the LW, we have introduced a variation in the radius of 10% for the fine mode, for the coarse mode and for both simultaneously. In any case, the differences observed in the radiative fluxes are below 1 $W \cdot m^{-2}$. By assuming an uncertainty in N of 10%, the variations in the fluxes are in the same range, always below 1 $W \cdot m^{-2}$. However, this differences translate in differences in the ARE_{LW} of 1.5 and 0.8 $W \cdot m^{-2}$ at the BOA and the TOA, which is relatively large considering that the obtained values range between 2.5-4.1 and 1.3-2.9 $W \cdot m^{-2}$. As discussed before, variations in the refractive index introduce variations in the ARF at the BOA of up to 1 and 0.6 $W \cdot m^{-2}$ at the TOA and the BOA respectively. Additionally, a strong influence of the LST on the $^{\uparrow}F_{LW}$ is observed, as will be discussed later on.
Page 19, line 25 onwards: *"On this latter day, larger differences are observed on the Net F_{LW} compared to 16 June, which might be explained by the inaccurate value of LST used due to the lack of precise data. A sensitivity test performed by increasing the air surface temperature measured at the meteorological station 5K indicates that the $^{\uparrow}F_{LW}$ increases its value up to 30 $W \cdot m^{-2}$ at the surface, and around 10 $W \cdot m^{-2}$ from 1 km onwards which is non-negligible. This would lead to an overestimation of the aircraft measured values, but still within a 6% difference. This highlights the need for accurate LST measurements for radiation simulations in the LW spectral range. Additionally, a sensitivity test performed by assuming a 10% uncertainty in the PSD parameters (r_{eff}, N and σ) leads to an estimated uncertainty of the F_{LW} retrieved by GAME of around 1.2 $W \cdot m^{-2}$. As stated before, the assumption of the refractive index can also introduce variations as large as 0.8 $W \cdot m^{-2}$. Considering the uncertainty of the pyrgeometer and the fact that the aircraft and the model present different vertical resolutions and time samplings and the uncertainties due to the use of the standard atmosphere or the parameterization of the surface properties the obtained differences are not significant."*

As the authors state, the CERES observations are too far in space (600 km) and in time (2 hours) to the surface observations, and a quantitative comparison with the RT model simulations is not possible. I think that the approximate results on the TOA fluxes using CERES data should be removed.

CERES data and related discussion have been removed from the manuscript.

Minor issues

Introduction: a quantitative description of the SW and LW dust radiative effect in the Mediterranean from previous studies is missing.

Additional information has been included in the introduction:

Page 2, lines18-25: *"The ARE in the Mediterranean region can be responsible for a strong cooling effect both at the surface (or bottom of the atmosphere, BOA) and the top of the atmosphere (TOA). The so-called forcing efficiency (FE), which is defined as the ratio between the ARE and the AOD, for the SW ranges between -150 and -160 W·m-2 for solar zenith angles (SZA) in the range 50-60° (di Biagio et al., 2009), being able to reach values larger than 200 W·m-2 at the BOA during strong dust events in the Mediterranean region (Gomez-Amo et al., 2011). The LW component accounts for an effect of up to 53% of the SW component and with an opposite sign (di Sarra et al. 2011; Perrone et al., 2012; Meloni et al. 2015)."*

Page 6, line 9: remove "diffuse" before downward radiative fluxes for the LW.

Done

Page 7, line 10: the authors should better explain how measurements corresponding to large pitch and roll aircraft angles are filtered. Moreover, this should be applied not only to downward pyrgeometer measurements, but to either pyranometers and pyrgeometers, both downward and upward-looking. The description of the correction of the ATR42 radiation measurements for the variation in the solar position and in the aircraft attitude during flight applies to pyranometers and not the pyrgeometer measurements, as stated in line 10. The final uncertainty in the airborne SW irradiance profiles is not reported.

The reviewer is right. This paragraph was referred to both pyranometers' and pyrgeometers' measurements. It has been modified.

Page 8, lines 23-24: a figure showing the airmass back trajectories may be useful.

Figure of the air mass trajectories will be added as supplementary material.

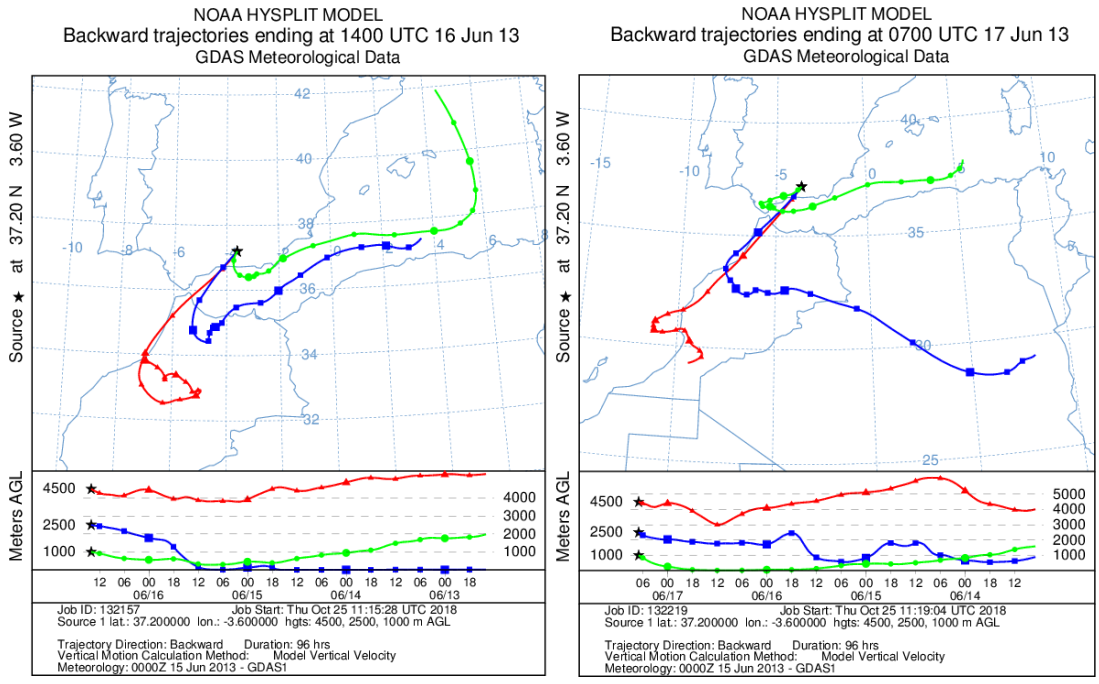

Page 8, line 26: change "profile" with "flight". Do the same at Page 9, line 5.

Done

Page 9, lines26-27: the authors mean that, due to the lack in MODIS data of LST the air temperature 2 m a.g.l. have been used as surrogate of the LST? This may lead to a relevant underestimation of the upward LW irradiance. Did the authors verify the differences in air and surface temperature in other cases and the impact of using one or the other in the simulation of the upward LW irradiances?

We performed a comparison between LST MODIS data and the air temperature at the meteorological station located at Granada experimental station using data corresponding to a 3-month period (May-July 2013). During daytime, the LST is on average 9.8 K larger than the surface air temperature around noon, when the satellites overpasses the station. At nighttime, the LST is 3.95 K lower than the surface air temperature. Considering the LST daily cycle and that the time of the flight was at 07:30UTC, we can expect a difference between the LST and the air temperature, but not as large as 9.8 K. A sensitivity test using the air temperature +5 K (which is the difference observed on June 16 between MODIS and the meteorological station) shows that the $^{\uparrow}F_{LW}$ increases its value up to 30 $W \cdot m^{-2}$ at the surface, and around 10 $W \cdot m^{-2}$ with increasing altitude (see attached figure). The effect on the ARF is however negligible at the BOA and it is 0.3 $W \cdot m^{-2}$ at the TOA.

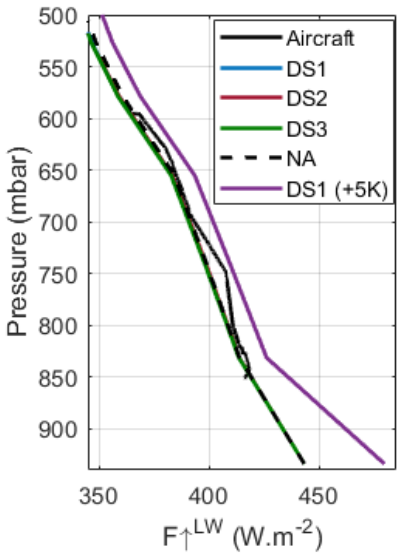

Page 13 lines 11-12: maybe the authors mean "extrapolation" instead of "interpolation" and "longer" instead of "shorter".

Text has been modified according to reviewers' suggestions.

Page 14 line 11: use "solar" and not "visible".

Done.

Page 15 line 2: the sentence "Even though the discrepancies in the AOD are within the uncertainty..." is misleading. DS1 and DS2 use AERONET AOD measurements as input, so both should agree within the measurement uncertainty (±0.01) at 550 nm. But a difference of 0.05 is reported in Table 4. This difference should be addressed and explained.

This sentence has been modified. In our case, the AOD indicated in Table 4 is not exactly the one provided by GRASP (extinction integral from surface to TOA), but the integral of the extinction profiles between the surface and the assumed as tops of the aerosol layers, which are the ones used as input for GAME

simulations. In the extinction profiles provided by GRASP, values above these tops are not exactly equal to zero, because GRASP assumed presence of stratospheric aerosols decreasing exponentially with the altitude (see Lopatin et al. 2013). For the comparison presented here we consider it is more accurate to consider only the region between the surface and the top of the aerosol layer so that we have homogenous criteria for the three datasets. Thus, a larger difference than the uncertainty is obtained between DS1 and DS2, since part of the GRASP extinction profiles (stratospheric aerosol) is not considered in the calculation of AOD.

Page 11, line 24 – Page 12, line 6: *"The AOD values presented here (included in Table 4) are obtained by integrating the α_{aer} profiles at 550 nm from the surface up to the considered top of the aerosol layer (4.3 km on June 16 and 4.7 km on June 17). In GRASP retrieved α_{aer} profiles, values above this top of the aerosol layer are slightly larger than zero since GRASP takes into account stratospheric aerosols by an exponential decay (Lopatin et al., 2013), thus the approach used here to calculate the AOD leads to lower values compared to the column-integrated AOD provided by the sun-photometer. Differences among the three datasets are more noticeable on June 16, when the AOD for DS1 is 0.05 lower than for DS2 and DS3, whereas on June 17 the maximum difference is 0.03, obtained between DS1 and DS2."*

Page 15 lines 5-7: the spectral variation of the SSA is provided only for the wavelengths at which it has been derived (Figure 4). For example DS3 from aircraft measurements is provided only for one wavelength. This not helps in understanding how optical properties may influence the SW radiation in the whole interval.

The values presented in Figure 4 correspond to the data obtained from the measurements which are used as input in the radiative transfer model. Unfortunately, the spectral variation of the SSA is not provided by the aircraft measurements. Anyway, this part of the manuscript has been rewritten in order to clarify it.

Page 15 lines 8-9: this sentence is rather obvious, since the comparison with aircraft radiation fluxes can be done only for the altitudes covered by the ATR42.

Removed.

Page 15 line 13: maybe the authors mean "below" instead of "above".

The reviewer is right; it has been modified.

Page 15 lines 25-28: the authors should present and discuss absolute and relative differences between measurements, AERONET calculations and GAME simulations. I don't understand the sentence stating that on 16 June the radiation presents large values (than 17 June?), please explain. An overestimation by 6% by GAME is much larger than the irradiance uncertainty. The estimation of the simulated irradiances is necessary in order to understand if such a difference is within the model and measurement respective uncertainties, otherwise it should be commented and possible causes addressed.

This part of the manuscript has been modified.

Page 17 lines 8-15: the SZA at which the RTM simulations are performed should be cleared. Are they those corresponding to the middle of the F30 and F31 flights (31.49◦ for 16 June and 61.93◦ for 17 June?). The SW ARE depends on the SZA, so when the authors presents the ARE from previous studies are they sure that such values can be direct compared with theirs? I don't think so, since results from Papadimas et al. (2012) are regional summer means. The same goes for the comparison with the other references (Sicard et al, 2014a,b; Barragan et al., 2017). Moreover, ARE depends on AOD. Thus, when comparing cases with different AOD, the radiative forcing efficiency (ARE per unit AOD) may be the most appropriate quantity.

The SZA used for the simulations is included in Table 4 (31.49º for 16 June and 61.93º for 17 June) and it does correspond to the middle of the flights. More information about the SZA is now added in the text. When comparing with previous studies the SZA is now taken into account. Moreover, the forcing efficiency is also included to ease the comparison with previous studies and avoid the dependence on the AOD values.

Page 18, line 7: change "diffuse" with "longwave".

Done.

Page 18, line 13: the upward and not the downward component of the LW irradiance depends on LST.

This part has been removed.

Page 30, Table 3: albedo in not defined in the LW region! Do authors refer to emissivity? Is it spectrally integrated or for a single wavelength?

It is the surface LW emissivity product provided by CERES, spectrally integrated in the range 4-100 μm. This information is now included in the manuscript.

Page 34, Figure 5: a shift is visible in the volume concentration profile of 17 June form GRASP code and aircraft measurements. Can the authors comment on it?

Details on the comparison between GRASP and the aircraft volume concentration profiles are already discussed in detail in Benavent-Oltra et al. (2017). The differences observed between both profiles are attributed to the different temporal sampling (the aircraft data provide instantaneous values whereas GRASP retrieval is performed using a 30-minutes averaged lidar profile) and the spatial separation (around 20 km distance between the aircraft and the lidar measurements), which can be associated to slight changes in the vertical distribution of the aerosol layers.

Page 35, Figure 6: The uncertainty range of the radiative fluxes from airborne instrumentation should be added in the plot to help understanding.

The estimated uncertainty for the airborne measured radiative fluxes is 5 $W \cdot m^{-2}$. Due to the horizontal scale used here to show the data, the uncertainty range is not visible in the plots.

A tracked version of the manuscript is included next. Changes made with respect to the previous version are underlined.

Impact of mineral dust on shortwave and longwave radiation: evaluation of different vertically-resolved parameterizations in 1-D radiative transfer computations

María José Granados-Muñoz[1], Michael Sicard[1,2], Roberto Román[3], Jose Antonio Benavent-Oltra[4,5], Rubén Barragán[1,2], Gerard Brogniez[6], Cyrielle Denjean[7,8], Marc Mallet[7], Paola Formenti[8], Benjamín Torres[6,9] and Lucas Alados-Arboledas[4,5]

[1] Remote Sensing Laboratory / CommSensLab, Universitat Politècnica de Catalunya, Barcelona, 08034, Spain
[2] Ciències i Tecnologies de l'Espai - Centre de Recerca de l'Aeronàutica i de l'Espai / Institut d'Estudis Espacials de Catalunya (CTE-CRAE / IEEC), Universitat Politècnica de Catalunya, Barcelona, 08034, Spain
[3] Grupo de Óptica Atmosférica (GOA), Universidad de Valladolid, Valladolid, Spain.
[4] Department of Applied Physics, University of Granada, 18071 Granada, Spain
[5] Andalusian Institute for Earth System Research (IISTA-CEAMA), University of Granada, Autonomous Government of Andalusia, 18006 Granada, Spain
[6] Laboratoire d'Optique Atmosphérique, University of Lille 1, Villeneuve d'Ascq, France
[7] CNRM, Centre National de la Recherche Météorologique (UMR3589, CNRS, Météo-France), Toulouse, France
[8] LISA, UMR CNRS 7583, Université Paris Est Créteil et Université Paris Diderot, Institut Pierre-Simon Laplace, Créteil, France
[9] GRASP-SAS, France

Correspondence to: Maria Jose Granados (maria.jose.granados@tsc.upc.edu)

Abstract.

Aerosol radiative properties are investigated in southeastern Spain during a dust event on June 16-17, 2013 in the framework of the ChArMEx/ADRIMED (Chemistry-Aerosol Mediterranean Experiment /Aerosol Direct Radiative Impact on the regional climate in the MEDiterranean region) campaign. Particle optical and microphysical properties from ground-based sun/sky photometer and lidar measurements, as well as in situ measurements onboard the SAFIRE ATR 42 French research aircraft are used to create a set of different levels of input parameterizations, which feed the 1-D radiative transfer model (RTM) GAME (Global Atmospheric ModEl). We consider three datasets: 1) a first parameterization based on the retrievals by an advanced aerosol inversion code (GRASP; Generalized Retrieval of Aerosol and Surface Properties) applied to combined photometer and lidar data; 2) a parameterization based on the photometer columnar optical properties and vertically-resolved lidar retrievals with the two-component Klett-Fernald algorithm; and 3) a parameterization based on vertically-resolved optical and microphysical aerosol properties measured in situ by the aircraft instrumentation. Once retrieved, the outputs of the RTM in terms of both shortwave and longwave radiative fluxes are compared against ground and in situ airborne measurements. In addition, the outputs of the model in terms of the aerosol direct radiative effect are discussed with respect to the different input parameterizations. Results show that calculated atmospheric radiative fluxes differ no more than 7 % to the measured ones. The three parameterization datasets produce a cooling effect due to mineral dust both at the surface and the top of the atmosphere. Aerosol radiative effects with differences up to 10 $W \cdot m^{-2}$ in the shortwave spectral range (mostly due to differences in the aerosol optical depth), and 2 $W \cdot m^{-2}$ for the longwave (mainly due to differences in the aerosol optical depth but also to the coarse

mode radius used to calculate the radiative properties) are obtained when comparing the three parameterizations. The study reveals the complexity of parametrizing 1-D RTMs as sizing and characterising the optical properties of mineral dust is challenging. The use of advanced remote sensing data and processing, in combination with closure studies on the optical/microphysical properties from in situ aircraft measurements when available, is recommended.

1 Introduction

The radiative effect by atmospheric aerosol is estimated to produce a net cooling effect of the Earth's climate. However, an accurate quantification of this cooling is extremely difficult. In fact, the aerosol radiative effect (ARE) is affected by large uncertainties. Due to the direct aerosol-radiation interaction, the ARE is estimated to be -0.27 W·m^{-2} on average at the global scale, with an uncertainty range of -0.77 to -0.23 W·m^{-2}, whereas the radiative effect related to cloud adjustments due to aerosols is -0.55 W·m^{-2} (-1.33 to -0.06 W·m^{-2}) (Boucher *et al.*, 2013), being the largest unknown in the radiative forcing of the atmosphere. The extent to which the ARE uncertainty range reported is due to physical processes or due to the measurement uncertainty itself is still hard to quantify.

In previous studies, the aerosol radiative effects in the longwave (LW) were commonly neglected due to the complexity of an accurate quantification of the optical properties in this spectral range (Roger et al., 2006; Mallet et al., 2008; Sicard et al., 2012). However, the contribution of the LW component to the ARE is non-negligible for large aerosol particles, i.e., marine aerosol or mineral dust (e.g. Markowicz et al., 2003; Vogelmann et al., 2003; Otto et al., 2007; Perrone and Bergamo, 2011; Sicard et al., 2014a,b; Meloni et al., 2018).

The contribution of mineral dust to the ARE in the infrared spectral range is especially relevant because of its large size and abundance (Meloni et al., 2018). Mineral dust is estimated to be the most abundant aerosol type in the atmosphere by mass (e.g., Ginoux et al., 2012; Choobari et al., 2014), with global emission between 1000 and 3000 Mt·yr^{-1} (Zender et al., 2003; 2004; Shao et al., 2011). The high temporal and spatial variability of dust concentrations and the variability in their microphysical and optical properties present a significant challenge to our understanding of how these particles impact the environment (Dubovik et al., 2002). Many measurements worldwide have been made using different approaches, including satellites which can provide global coverage of mineral dust properties. However, the retrievals of particle properties are still affected by large uncertainties (Levy et al., 2013) and the information on mineral dust properties is quite scarce (Formenti et al., 2011).

One of the areas frequently influenced by mineral dust is the Mediterranean Sea region, affected by dust intrusions from the close Sahara Desert or the Middle-East region (Moulin et al., 1998; Israelevich et al., 2012; Gkikas et al., 2013) producing significant perturbations to the shortwave (SW) and the LW radiation balance (di Sarra et al. 2011; Papadimas et al., 2012; Perrone et al., 2012; Meloni et al. 2015) as well as the regional climate (Nabat et al., 2015). The ARE in the Mediterranean region can be responsible

for a strong cooling effect both at the surface (or bottom of the atmosphere, BOA) and the top of the atmosphere (TOA). The so-called forcing efficiency (FE), which is defined as the ratio between the ARE and the aerosol optical depth (AOD), for the SW ranges between -150 and -160 $W \cdot m^{-2}$ for solar zenith angles (SZA) in the range 50-60° (di Biagio et al., 2009), being able to reach values larger than 200 $W \cdot m^{-2}$ at the BOA during strong dust events in the Mediterranean region (Gomez-Amo et al., 2011). The LW component accounts for an effect of up to 53% of the SW component and with an opposite sign (di Sarra et al. 2011; Perrone et al., 2012; Meloni et al. 2015).

The Aerosol Direct Radiative Impact on the regional climate in the MEDiterranean region (ADRIMED) field campaign within the Chemistry-Aerosol Mediterranean Experiment (ChArMEx, http://charmex.lsce.ipsl.fr) took place in the Mediterranean region from 11 June to 5 July 2013 (Mallet et al., 2016). It aimed at characterizing the different aerosol particles and their radiative effects using airborne and ground-based measurements collected in the Mediterranean Basin, with special focus on the western region. In particular, two ChArMEx/ADRIMED flights, F30 and F31, from the French ATR 42 environmental research aircraft of SAFIRE (http://www.SAFIRE.fr), took place above southeastern Spain during a Saharan dust episode on 16 and 17 June 2013.

In this paper, we present an analysis of the mineral dust radiative properties during this particular episode taking advantage of the thorough database available. Multiple datasets are used as input in a radiative transfer model (RTM) to evaluate the influence of the different measurements and data processing in the retrieved direct ARE. The model used here is the Global Atmospheric ModEl (GAME; Dubuisson et al., 1996; 2005), which allows calculating both the solar and thermal infrared fluxes. An evaluation against aircraft in situ measurements of radiative fluxes is also presented.

Two main goals are pursued: i) the quantification of the direct ARE for two case studies within a dust transport episode and ii) the evaluation of the model estimates sensitivity to the aerosol input used.

The paper is structured as follows: Section 2 includes a description of both the ground-based and in situ aircraft instrumentation and a short description of the retrieval algorithms used for the present study; Section 3 is devoted to the description of GAME and the input datasets used here and results are presented in Section 4; finally, a short summary and concluding remarks are included in Section 5.

2 Instruments and data

2.1 Ground-based measurements

Ground-based measurements used in this work were carried out at the Andalusian Institute for Earth System Research (IISTA-CEAMA) of the University of Granada, Spain (37.16º N, 3.61º W, 680 m a.s.l.) by the Atmospheric Physics Group of the University of Granada (GFAT-UGR). This experimental site is located in the western Mediterranean basin, near the African continent (~200 km). Therefore, long-range transport of mineral dust particles from North Africa is a main source of natural atmospheric aerosol in the region (e.g. Lyamani et al., 2005; Valenzuela et al., 2012). The station is also affected by long-range transported

smoke (Ortiz-Amezcua et al., 2017) and fresh smoke from nearby biomass burning (Alados-Arboledas et al., 2011). Anthropogenic sources such as pollution from Europe, the Iberian Peninsula and the Mediterranean Sea (Pérez-Ramírez et al., 2016) also affect the station. Local sources are mainly road traffic and central heating systems (Titos et al., 2017).

IISTA-CEAMA station is equipped with a CE-318-4 (*Cimel Electronique*) sun/sky photometer which belongs to the AERONET network (Holben et al., 1998). This instrument makes direct solar irradiance measurements, used to derive aerosol optical depth (AOD), and sky radiance measurements both at least at the following nominal wavelengths (λ): 440, 670, 870 and 1020 nm. The AOD product provided by AERONET have an uncertainty of ±0.01 for $\lambda > 440$ nm and of ±0.02 for $\lambda < 440$ nm (Holben et al., 1998; Eck et al., 1999). AERONET also provides aerosol optical and microphysical properties such as columnar particle size distribution (PSD), real and imaginary parts of the refractive indices (RRI and IRI, respectively), asymmetry factor (*g*) and single scattering albedo (SSA), using the AOD and sky radiance values in an inversion algorithm (Dubovik and King, 2000; Dubovik et al., 2006). For the present study, AERONET Version 2 Level 1.5 (Level 2.0 when available) data are used. The uncertainty in the retrieval of SSA is ±0.03 for high aerosol load ($AOD_{440} > 0.4$) and solar zenith angle (SZA) > 50º; while for measurements with low aerosol load ($AOD_{440} < 0.2$), the retrieval accuracy of SSA drops down to 0.02–0.07 (Dubovik and King, 2000). For high aerosol load and SZA > 50°, errors are about 30%–50% for the IRI. For particles in the size range $0.1 < r < 7$ μm (being r the aerosol radius), errors in PSD retrievals are around 10–35%, while for sizes lower than 1 μm and higher than 7 μm retrieval errors rise up to 80–100%. The inversion code provides additional variables such as the volume concentration, effective radius, r_{eff}, and geometric standard deviation of the equivalent lognormal distribution, σ, for fine and coarse modes of the retrieved PSD which will be used in the current study.

The multi-wavelength aerosol Raman lidar MULHACEN, based on a customized version of LR331D400 (Raymetrics S.A.), is operated at Granada station as part of EARLINET/ACTRIS (European Aerosol Research Lidar Network / Aerosols, Clouds, and Trace Gases Research Infrastructure Network; https://www.actris.eu/default.aspx; Pappalardo et al., 2014) since April 2005. The system has a monostatic biaxial configuration, which usually requires an overlap correction to minimize the incomplete overlap effect (Navas-Guzmán et al., 2011). The system emits vertically to the zenith by means of a pulsed Nd:YAG laser with 2nd- and 3rd-harmonic generators, that emits simultaneously at 1064, 532 and 355 nm. The receiving system consists of several detectors, which can split the radiation according to the three elastic channels at 355, 532 (parallel- and perpendicular-polarized; Bravo-Aranda et al., 2013), and at 1064 nm; two nitrogen Raman channels at 387 and 607 nm; and a water vapor Raman channel at 408 nm (Navas-Guzmán et al., 2014). The aerosol backscatter coefficient profiles ($\beta_{aer}(z,\lambda)$, being z the vertical height) obtained from the multi-wavelength lidar were calculated with the Klett-Fernald method (Fernald et al., 1972; Fernald, 1984; Klett, 1981, 1985). For the retrieval of the aerosol extinction coefficient profiles ($\alpha_{aer}(z,\lambda)$), a height-independent lidar ratio (LR) obtained by forcing the vertical integration of $\alpha_{aer}(z,\lambda)$ to

the AOD from AERONET photometer (Landulfo et al., 2003) was assumed. The assumption of a constant LR introduces uncertainty in $\alpha_{aer}(z,\lambda)$ retrievals, especially when different types of aerosol appear at different layers. In our case, the LR used for the Klett-Fernald retrieval are very similar to those provided by GRASP (see Benavent-Oltra et al., 2017). Considering the different uncertainty sources, total uncertainty in the profiles obtained with Klett-Fernald method is usually 20% for $\beta_{aer}(z,\lambda)$ and 25-30% for $\alpha_{aer}(z,\lambda)$ profiles (Franke et al., 2001).

Additionally, surface temperature and pressure are continuously monitored at IISTA-CEAMA by a meteorological station located 2 m above the ground. At the same location, the global and diffuse downward radiative fluxes for the SW are continuously measured with a CM11 pyranometer (Kipp & Zonen) and diffuse downward radiative fluxes for the LW are measured with a PIR pyrgeometer (Eppley), being both instruments regularly calibrated at the site (Antón et al., 2012, 2014).

2.2 Airborne measurements

The Safire ATR 42 aircraft performed two overpasses above Granada on June 16 (flight F30) and 17 (flight F31) in 2013 during the ChArMEx/ADRIMED campaign. During F30, the SAFIRE ATR 42 descended performing a spiral trajectory from 14:15 to 14:45 UTC, whereas during flight F31, the aircraft ascended in the early morning (from 07:15 to 07:45 UTC) at around 20 km from Granada station (see Fig. 1 from Benavent-Oltra et al., 2017). Additional flight details can be found in previous studies (Denjean et al., 2016; Mallet et al., 2016; Benavent-oltra et al., 2017; Román et al., 2018).

The airborne instrumentation includes a Scanning Mobility Particle Sizer (SMPS) and an Ultra-High Sensitivity Aerosol Spectrometer (UHSAS), for measuring aerosol number size distribution in the submicron range. The Forward Scattering Spectrometer Probe model 300 (FSSP-300) and the GRIMM OPC (sky-OPC 1.129) were used to measure the optical size distributions in the diameter nominal size range between 0.28 and 20 μm and between 0.3 and 32 μm, respectively. A nephelometer (TSI Inc, model 3563) was used to measure the particle scattering coefficient at 450, 550 and 700 nm, and a Cavity Attenuated Phase Shift (CAPS-PMex, Aerodyne Inc.), was employed to obtain the aerosol extinction coefficient (α_{aer}) at 530 nm. For more details on the aircraft instrumentation see Denjean et al. (2016) and references therein. The PLASMA (Photomètre Léger Aéroporté pour la Surveillance des Masses d'Air) system, which is an airborne sun-tracking photometer, was additionally used to obtain AOD with wide spectral coverage (15 channels between 0.34 – 2.25 μm) with an accuracy of approximately 0.01, as well as the vertical profiles of the aerosol extinction coefficient (Karol et al., 2013; Torres et al., 2017).

Airborne radiative fluxes (F) were measured with Kipp & Zonen CMP22 pyranometers and CGR4 pyrgeometers. Upward and downward SW fluxes ($^{\uparrow}F_{SW}$ and $^{\downarrow}F_{SW}$) were measured in the spectral range 297-3100 nm by two instruments located above and below the aircraft fuselage. The same setup was used for the pyrgeometers, which provided the LW upward and downward radiative fluxes ($^{\uparrow}F_{LW}$ and $^{\downarrow}F_{LW}$) for wavelengths larger than 4 μm. Both pyranometers and pyrgeometers were calibrated in January 2013 and

data were corrected for the temperature dependence of the radiometer's sensitivity following Saunders et al. (1992).

Radiation measurement data from the aircraft were filtered out for large pitch and roll angles and corrected from the rapid variations of the solar incidence angle around the solar zenith angle due to the aircraft attitude (pitch and roll). This correction also depends on aircraft heading angle and solar position. It should be noted that, beforehand, roll and pitch offsets must be determined (the axis sensor is not necessarily vertical on average during a horizontal leg). Cosine errors were taken into account. Finally, data were corrected from variations of the SZA during the flight to ease the comparison with GAME retrievals. After these various corrections, an estimated uncertainty of ±5 $W \cdot m^{-2}$ is considered to affect the data, taking into account the accuracy of the calibration and of the acquisition system together with the consistency of airborne measurements (Meloni et al., 2018).

2.3. The GRASP code

The GRASP (Generalized Retrieval of Aerosol and Surface Properties) code (Dubovik et al., 2011, 2014), provides aerosol optical and microphysical properties in the atmosphere by combining the information from a variety of remote sensors (e.g. Kokhanovsky et al., 2015; Espinosa et al., 2017; Torres et al., 2017; Román et al., 2017, 2018; Chen et al., in review). In our case, GRASP was used to invert simultaneously coincident lidar data (range corrected signal, RCS, at 355, 532 and 1064 nm) and sun/sky photometer measurements (AOD and sky radiances both from AERONET at 440, 675, 870 and 1020 nm) providing a detailed characterization of the aerosol properties, both column-integrated and vertically-resolved. It is worthy to note that this GRASP scheme, based on Lopatin et al. (2013), presents the main advantage that it allows retrieving aerosol optical and microphysical properties for two distinct aerosol modes, namely fine and coarse. The α_{aer}, β_{aer}, SSA (all at 355, 440, 532, 675, 870, 1020 and 1064 nm), and aerosol volume concentration (VC) profiles obtained as output from GRASP will be used as input to GAME in the present study, together with the column-integrated PSD properties (namely r_{eff} and σ for fine and coarse modes). A more in-depth analysis of GRASP output data retrieved using the lidar and sun/sky photometer data at Granada station for the two inversions simultaneous to the aircraft overpasses during flights F30 and F31 during ChArMEx/ADRIMED campaign can be found in Benavent-Oltra et al. (2017).

3. GAME radiative transfer model

3.1. GAME description

The GAME code is widely described by Dubuisson et al. (2004; 2005) and Sicard et al. (2014a). It is a modular RTM that allows calculating upward and downward radiative fluxes at different vertical levels from the ground up to 20 km (100 km) in the SW (LW) spectral range. The solar and thermal infrared fluxes are calculated in two adjustable spectral ranges, which in this study were fixed to match those of the aircraft

radiation measurements, namely 297 - 3100 nm for the SW and 4.5 – 40 μm for the LW, by using the discrete ordinates method (Stamnes et al., 1988). Note that the GAME code has a variable spectral sampling in the SW (depending on the spectral range considered) and a fixed spectral sampling (115 values) in the LW spectral range (Table 1).

[Table 1]

3.2. GAME input data parameterization

The two considered SAFIRE ATR 42 flights, F30 and F31, took place on 16 and 17 June 2013, respectively, simultaneously to ground-based lidar and sun/sky photometer measurements performed at the station. On these days, mineral dust with origin in the Sahara region (southern Morocco near the border with Algeria) reached Granada after ~4 days of travelling, according to back-trajectories analysis (not shown) and the results presented in Denjean et al. (2016). A homogenous dust layer reaching up to 5 km agl was observed on June 16, whereas on June 17 the dust layer was decoupled from the boundary layer and located between 2 and 4.5 km agl (Benavent-Oltra et al., 2017). A similar structure was observed also above Minorca (Renard et al., 2018), which is an indicator of the horizontal extension of the dust event. On June 16, the F30 flight above Granada site took place between 14:15 and 14:45 UTC in coincidence with the lidar measurements. The corresponding SZA at 14:30UTC was 31.49º. The sun/sky photometer microphysics data were not available till 16:22 UTC, even though the retrieved AOD and its spectral dependence (represented by the Angström exponent) were very stable between the time of the lidar measurements and the time of the sun/sky photometer inversion. On June 17, the F31 flight occurred in the early morning (07:15 to 07:45 UTC, with SZA=61.93º at 07:30UTC), and simultaneous lidar and sun/sky photometer were available. Unfortunately, the airborne vertical profile of extinction by the CAPS measurements was not available during this second flight. Clouds were detected by the lidar on June 17 after 15:00 UTC. Furthermore, a sky-camera and the ground-based pyranometer and pyrgeometer data indicate cloud contamination (but not in the zenith) in the radiation data much earlier (around 09:00 UTC), preventing also satellite retrievals in the region.

A summary of the experimental data used as input for GAME calculations during these two case studies is presented in Table 2. This input includes namely surface parameters and atmospheric profiles of meteorological variables, main gases concentrations and aerosol properties. The aerosol properties used in the present study are parameterized using three different datasets, based on the different instrumentation and retrievals available, i.e. Dataset 1 (DS1), Dataset 2 (DS2) and Dataset 3 (DS3). A more detailed description of the different parameters is provided next.

[Table 2]

3.2.1. Surface parameters and profiles of meteorological variables

The surface parameters required for GAME are the surface albedo (*alb*(λ)) and land-surface temperature (LST). The *alb*(λ) for the SW range is obtained from the sun/sky photometer data using the AERONET

retrieval at 440, 675, 880 and 1020 nm, and for the LW from the integrated emissivity between 4 and 100 μm provided by the Single Scanner Footprint (SSF) Level2 products of the CERES (Clouds and the Earth's Radiant Energy System; (http://ceres.larc.nasa.gov/) instrument (Table 3). LST values are obtained from MODIS (Moderate Resolution Imaging Spectroradiometer) 1-km daily level-3 data (Wan et al., 2014) on June 16. Unfortunately, on June 17 MODIS data were not available due to the presence of clouds and the local surface temperature was obtained from temperature measurements at Granada site, where the meteorological station is located at 2 m above the ground. LST and $alb(\lambda)$ values used for the two analyzed cases are included in Table 3.

[Table 3]

Figure 1 shows the pressure (P), temperature (T), and relative humidity (RH) profiles obtained from the SAFIRE ATR 42 measurements. Data from the meteorological station located at IISTA-CEAMA are used to complete these profiles at the surface level, whereas at altitudes above the aircraft flight, a scaled US standard atmosphere is used for completion. The concentration profiles of the main absorbing gases (O_3, CH_4, N_2O, CO and CO_2) are also taken from the US standard atmosphere, while for the gaseous absorption coefficients the HITRAN database is used (as in Sicard et al., 2014a; 2014b).

[Figure 1]

3.2.2. Aerosol parameterization

As for the aerosol parameterization, $\alpha_{aer}(\lambda,z)$, SSA(λ,z) and $g(\lambda,z)$ are required as GAME input data (Table 2). For the SW wavelengths, these properties can be obtained from the measurements performed with the instrumentation available during the campaign; namely the lidar, the sun/sky photometer and the in situ instrumentation onboard the aircraft. On the other hand, direct measurements of the aerosol properties in the LW are not so straightforward and thus scarce. Hence, the aerosol LW radiative properties are calculated by a Mie code included as a module in GAME. According to Yang et al. (2007), the dust particles non-sphericity effect at the thermal infrared wavelengths is not significant on the LW direct ARE, thus the shape of the mineral dust can be assumed as spherical for the Mie code retrievals introducing negligible uncertainties.

For the SW simulations, we run GAME using three different aerosol input datasets, i.e. DS1, DS2 and DS3 (Table 2), in order to evaluate their influence on the ARE calculations. DS1 relies on a parameterization based on the advanced post-processing GRASP code, which combines lidar and sun/sky photometer data to retrieve aerosol optical and microphysical properties profiles; DS2 relies on Klett-Fernald lidar inversions and AERONET products and corresponds to a reference parameterization (easily reproducible at any station equipped with a single- or multi-wavelength lidar and an AERONET sun/sky photometer and without the need of an advanced post-processing algorithm); and DS3 relies on in situ airborne measurements and corresponds to an alternative parameterization to DS1 and DS2.

Figure 2 shows α_{aer} profiles on June 16 (top) and 17 (bottom) obtained using the three different approaches. For DS1 (Figure 2a and d), α_{aer} profiles at seven different wavelengths obtained with GRASP

are used as input data in GAME. In DS2 (Figure 2b and 3e), the α_{aer} profiles are obtained from the lidar data using Klett-Fernald retrievals and adjusting the lidar ratio to the AERONET retrieved AODs, as mentioned in Section 2.1. Finally, for DS3 the α_{aer} values are obtained from the aircraft in situ measurements (CAPS and PLASMA data on June 16 and PLASMA on June 17). A detailed analysis and discussion on the comparison between α_{aer} profiles provided by the aircraft measurements, GRASP and the lidar system at Granada is already included in Benavent-Oltra et al. (2017). In general, the lidar, GRASP and the CAPS data are in accordance, observing the same aerosol layers and similar values, with differences within 20%. GRASP slightly overestimates CAPS data by 3 Mm^{-1} on average, whereas the differences with PLASMA are larger, reaching a 30% (or 11 Mm^{-1}). In the case of the Klett-Fernald retrieval, values are lower than those retrieved with GRASP by up to 19%. Considering that the uncertainty in α_{aer} is around 30% for both GRASP and the Klett-Fernald retrieval and 3% for the CAPS data, this discrepancy is well below the combined uncertainty of the different datasets. Differences in the α_{aer} profiles translate into differences in the integrated extinction and, hence, in differences in the AOD values used as input in the radiative fluxes retrievals. The AOD values presented here (included in Table 4) are obtained by integrating the α_{aer} profiles at 550 nm from the surface up to the considered top of the aerosol layer (4.3 km on June 16 and 4.7 km on June 17). In GRASP retrieved α_{aer} profiles, values above this top of the aerosol layer are slightly larger than zero since GRASP takes into account stratospheric aerosols by an exponential decay (Lopatin et al., 2013), thus the approach used here to calculate the AOD leads to lower values compared to the column-integrated AOD provided by the sun-photometer. Differences among the three datasets are more noticeable on June 16, when the AOD for DS1 is 0.05 lower than for DS2 and DS3, whereas on June 17 the maximum difference is 0.03, obtained between DS1 and DS2. The AOD values at 550 nm reveal that GRASP input data (DS1) and in a lesser extent the aircraft in situ data (DS3) underestimate the aerosol load in the analyzed dust layer compared to AERONET (DS2) due to the differences in the retrieval techniques, e.g. whereas AERONET provides integrated AOD for the whole column, low α_{aer} values above the aerosol layer are neglected for the AOD calculations in DS1 and DS3.

[Figure 2]

[Table 4]

Figure 3 presents the SSA values retrieved by GRASP algorithm, used as input for GAME in DS1, on June 16 (F30, Figure 3a) and 17 (F31, Figure 3b). The mean SSA at 440 nm is equal to 0.92 on June 15, whereas on June 17 is 0.85. On June 17 the SSA profiles present lower values and more variation with height than on June 16; the lower SSA values indicate the presence of more absorbing particles on June 17. The vertical variation on June 17 is associated to the presence of two different layers, whereas a more homogeneous dust layer is observed on June 16. For DS2, the SSA are taken from AERONET columnar values and assumed to be constant with height (Figure 4a). The SSA at 440 nm was 0.89 and 0.83 on June 16 and 17 respectively, as already observed in Figure 3, SSA values are lower on June 17 due to the intrusion of more absorbing particles. For DS3, SSA values at 530 nm are obtained from the nephelometer and the CAPS or PLASMA onboard the ATR. In order to reduce the uncertainty of the measured data, only averaged values for the column will be considered, being 0.88 and 0.83 on June 16 and June 17 (Figure 4). Therefore, differences of up to 0.04 and 0.02 are observed on June 16 and 17 respectively among the SSA values obtained with the three datasets. Despite these difference, the retrieved SSA values obtained here are within the range of typical values for dust aerosols (Dubovik et al., 2002; Lopatin et al., 2013) and differences are still within the uncertainty limits, which range between 0.02 and 0.07 depending on the aerosol load for AERONET data (Dubovik et al., 2000) and is 0.04 for the aircraft values. In the case of *g* values, the same data are used for the three aerosol input datasets. Multispectral values of *g* are taken from AERONET columnar values and assumed to be constant with height (Figure 4b).

[Figure 3]

[Figure 4]

Summing up, for the SW aerosol parametrization in GAME three datasets are tested. In DS1, GRASP provided spectral profiles at 7 wavelengths of the aerosol extinction and SSA are used. In DS2, the Klett retrieved extinction profiles at 3 wavelengths are used together with the AERONET SSA columnar values at 4 wavelengths, which are assumed to be constant with height. For DS3, one extinction profile at 550 nm and a column-averaged single-wavelenght value of the SSA from the airborne measurements are considered. In the three cases, the column-integrated AERONET asymmetry parameter at 4 wavelengths is assumed to be constant with height and used as input.

For the LW calculations, the Mie code is used to obtain $\alpha_{aer}(\lambda,z)$, SSA(λ,z) and g(λ,z) from the information on the aerosol PSD, complex refractive index (RI) and density, following a similar approach to that used in previous studies (Meloni et al., 2015; 2018; Peris-Ferrús et al., 2017). A summary of the aerosol parameters used in the Mie calculations is included in Table 5. Three different datasets are also used for the aerosol parameterization in the LW calculations. In this case, the sensitivity of the model to the PSD used is tested. A similar scheme to that presented for the SW is used, where DS1 relies on GRASP retrievals, DS2 on AERONET products and DS3 relies on in situ airborne measurements.

[Table 5]

The spectral real and imaginary parts of the RI of mineral dust in the LW are obtained from Di Biagio et al. (2017), using the Morocco source, and assumed constant with height. The analysis by Di Biagio et al. (2017) only covers the spectral range 3-16 μm, so an extrapolation assuming the spectral dependence presented in Krekov (1993) for shorter and longer wavelengths is performed. This assumption is not exempt of uncertainty, since the refractive index present a certain variability associated to the different nature of mineral dust properties. For example, the use of the refractive index provided for the Algerian and Mauritanian sources from Di Biagio et al., (2017) leads to variations in the ARF of 0.8 and 0.3 $W \cdot m^{-2}$ at the BOA and the TOA respectively. Additionally, vertical variations of the refractive index are also a source of uncertainty in the obtained radiative fluxes. The mineral dust particle density is assumed to be 2.6 $g \cdot cm^{-3}$ (Hess et al., 1998). Regarding the PSD, three parameters (namely the effective radii, r_{eff}, standard deviation, σ, and the numeric concentrations, *N*) for fine and coarse modes are used. The fine mode comprises particles within the diameter range 0.1–1 μm, whereas for the coarse mode the range 1-30 μm is considered. In the case of DS1, *N* values are obtained from the volume concentration profiles provided by GRASP assuming spherical particles in the range between 0.05 and 15 μm radii (Figure 5). Values of r_{eff} and σ provided by GRASP (Table 4) are column-integrated and thus assumed to be constant with height. This is the case also for DS2, in which the PSD parameters are column-integrated values provided by the AERONET retrieval in Granada (see Table 4).

[Figure 5]

For DS3, the volume concentration (or the equivalent *N*), *r* and σ profiles for the fine and coarse modes (Figure 5) are calculated from the data provided by the aircraft in situ measurements in the range between 0.02 and 40 μm diameter. Benavent-Oltra et al. (2017) found a general good accordance between the

volume concentration profiles measured by the instrumentation onboard the SAFIRE ATR 42 and retrieved with GRASP, with differences in the total volume concentration profiles for the dust layers lower than 8 $\mu m^{-3} \cdot cm^{-2}$ (20%), which fall within the combined uncertainty. Nonetheless differences are still noticeable, especially in the fine mode. On June 17, GRASP overestimates the aircraft measurements for the fine mode and underestimates them for the coarse mode, which in turns results in a quite different fine to coarse concentration ratio for DS1 and DS3. Additionally, a slight shift is observed in the vertical structure of the aerosol layers. Differences are mostly technical, i.e., GRASP retrieval is based on 30-min averaged lidar profiles while the aircraft provide instantaneous measurements, but they can be also partially caused by the discrepancies between the vertical aerosol distribution above Granada (sampled by the lidar) and the concentration measured during the aircraft trajectory as they are not exactly coincident. In addition, for June 16, there is a 2 hours' time difference between the sun/sky photometer retrieval used in GRASP calculations and the airborne measurements which can lead to slight differences in the aerosol properties despite the homogeneity of the dust event during this period. In the following, we quantify the impact these differences may introduce in the calculations of F.

3.2.3. GAME output data

As a result of the simulation, GAME provides vertical profiles of radiative fluxes in the shortwave (F_{SW}) and longwave (F_{LW}) spectral ranges. The net flux can be calculated from the obtained profiles for both spectral ranges as:

$$\text{Net } F = {}^{\downarrow}F - {}^{\uparrow}F \qquad \textbf{Equation 1}$$

where the upward and downward arrows are for upward and downward fluxes respectively. From the obtained radiative fluxes profiles, the direct ARE profiles are calculated according to the following equation:

$$ARE = ({}^{\downarrow}F^{w} - {}^{\uparrow}F^{w}) - ({}^{\downarrow}F^{o} - {}^{\uparrow}F^{o}) \qquad \textbf{Equation 2}$$

where F^w and F^o are the radiative fluxes with and without aerosols, respectively. The direct ARE can be obtained for the SW (ARE_{SW}) and the LW (ARE_{LW}) spectral ranges.

4 Mineral dust effect on shortwave and longwave radiation

4.1. SW radiative fluxes

Figure 6 shows the radiative fluxes profiles for the SW spectral range obtained with GAME using the three different input datasets described in Section 3, as well as the Net F_{SW}. The radiative fluxes measured by the pyranometer onboard the SAFIRE ATR 42 are also included in the figure. The three GAME simulations show similar values with differences below 8 $W \cdot m^{-2}$ on average, which represents less than 1% variation. The differences in the obtained fluxes are mostly due to the differences in the aerosol load considered depending on the inputs. Even though the differences in the AOD among the different datasets are small

(lower than 0.05), they can lead to differences in F_{SW} and ultimately in the ARE_{SW}. In order to quantify these differences, we performed a sensitivity test by varying the AOD while the other parameters were kept constant. We observed a maximum variation in the F_{SW} of 6.5 $W \cdot m^{-2}$ (0.7%) at the surface, decreasing with height, for changes in the AOD of up to 0.05, which is the difference we observe between the AOD for DS2 and DS1 on June 16. This result partly explains the differences among the three datasets. In addition, a sensitivity test performed by varying exclusively the SSA indicates that more absorbing particles are related to less $^{\downarrow}F_{SW}$ at the surface, namely a variation of 1% is observed at the BOA for a decrease in the SSA of 0.03. The influence of the SSA decreases with height being negligible at the TOA. For the $^{\uparrow}F_{SW}$, a decrease of 0.8% is observed at the BOA if more absorbing particles are present, but in this case the influence at the TOA is larger (2.2%). In our case, the larger AOD assumed for DS2 on both days (see Table 4 and Figure 2), causes the $^{\downarrow}F_{SW}$ to be slightly lower compared to DS1. For DS3 the AOD is similar to DS2, but the SSA values used, which are relatively smaller compared to those measured by AERONET (see Figure 4), lead to lower values of the radiative fluxes than for DS2. The vertical distribution of the SSA also influences the radiative fluxes in the SW as demonstrated in previous studies (Gomez-Amo et al., 2010; Guan et al., 2010), contributing to explain the differences observed among the three datasets analyzed here.

The evaluation against the aircraft measurements shows larger differences for altitudes below 2.5 km (~860 mbar) on June 16, whereas a better agreement is found above. On June 17, no $^{\uparrow}F_{SW}$ aircraft data are available below 2 km. Relative differences between the model and the aircraft measured data (calculated as $(F_{GAME}-F_{aircraft})/F_{aircraft}$) are well below 7%, being the largest discrepancies observed for the $^{\downarrow}F_{SW}$. Differences among the three GAME outputs and the aircraft pyranometer are lower than 5% for the Net F_{SW} on both days. Considering the very different approaches followed by the model and the direct measurements by the airborne pyranometer (i. e. vertical resolution, temporal sampling and data acquisition and processing), together with the uncertainty of the pyranometer (5 $W \cdot m^{-2}$) and the estimated uncertainty of the model outputs, which can be as large as 19 $W \cdot m^{-2}$) these differences are quite reasonable. A conclusive result on which input dataset provides a better performance is unlikely because of the similar results obtained with the three datasets.

[Figure 6]

The values at the surface (or bottom of the atmosphere, BOA) and at the top of the atmosphere (TOA) for the different radiative fluxes can be also evaluated against different instruments: measurements for the $^{\downarrow}F_{SW}$ at the surface are available from the sun-photometer; AERONET provides values of the $^{\downarrow}F_{SW}$ and $^{\uparrow}F_{SW}$ at both the BOA and the TOA. The time series for these measurements corresponding to 16-17 June and the results obtained with GAME for the different datasets are shown in Figure 7. AERONET surface radiative fluxes have been extensively validated at several sites around the world (e.g. Garcia et al., 2008) and, in addition, all AERONET sun-photometers are mandatorily calibrated once a year. Thus, in order to compare GAME results with AERONET data, we have performed additional simulations for the

time of the closest AERONET measurement on June 16 (at 16:22UTC), assuming that the aerosol parameterization is constant with time between the flight time and the photometer measurement. $^{\downarrow}F_{SW}$ values at the surface obtained with GAME are 564.8, 551.8 and 547.0 W·m^{-2} for DS1, DS2 and DS3 respectively, very similar to the 531.4 W·m^{-2} provided by AERONET. On June 17, GAME simulations at 07:40UTC (instead of 07:30UTC, which is the time of the flight), provide $^{\downarrow}F_{SW}$ at the surface of 466.3, 468.3 and 456.4 W·m^{-2}, very close to the AERONET value of 463.7 W·m^{-2}.

At the TOA, the $^{\uparrow}F_{SW}$ between GAME and AERONET are in quite good agreement on both days. On June 16, the $^{\uparrow}F_{SW}$ obtained with GAME simulations is equal to 152.0, 153.0 and 148.5 W·m^{-2} and with AERONET is equal to 146.2 W·m^{-2}. On June 17, the obtained values with GAME are 133.6, 136.6 and 130.9 W·m^{-2} for DS1, DS2 and DS3 and 131.6 W·m^{-2} for AERONET.

[Figure 7]

The ARE_{SW} profiles, calculated by using Eq. 2 and GAME simulations for the three input datasets are shown in Figure 8, together with the simultaneous values provided by AERONET on 17 June at the BOA and TOA. Comparing the three GAME simulations, we can see that the low discrepancies in the F profiles from Figure 6 lead to variations in the ARE_{SW} of 10-27% (3-10 W·m^{-2}) over the averaged profile depending on the input dataset used. The variations in the ARE_{SW} are tightly connected to differences in the AOD considered as input in the model, as already observed in previous studies (Sicard et al., 2014a; Lolli et al., 2018; Meloni et al., 2018). The SSA and the vertical distribution of the aerosol also plays an important role, as observed for DS3, which shows a profile quite different from DS2 despite the AOD being quite close for both datasets.

Differences are also observed when comparing ARE_{SW} values obtained from GAME to those retrieved by AERONET. Contrary to GAME simulations, AERONET does not consider the vertical distribution of the aerosols when calculating the ARE_{SW}, and the definition of the ARE_{SW} at the BOA ($^{BOA}ARE_{SW}$) is slightly different. Indeed, AERONET $^{BOA}ARE_{SW}$ is calculated as the difference between the downward fluxes with and without aerosols, the difference between the upward fluxes (reflected by the Earth) being neglected. Considering this, we can correct the $^{BOA}ARE_{SW}$ provided by AERONET multiplying by a factor (1- $alb(\lambda)$). The corrected $^{BOA}ARE_{SW}$ value on 17 June is thus -31.9 W·m^{-2}, which is within the range of values provided by GAME at the surface. All discrepancies observed here are mostly intrinsic to the different techniques used for the acquisition of the data and the retrieval algorithms. The effect of the data processing has also been observed in previous studies (Lolli et al., 2018). Moreover, the sensitivity tests performed reveal that an increase in the AOD of 0.05 can lead to a stronger effect of the ARE both at the BOA (up to 6.7 W·m^{-2}) and the TOA (up to 2.5 W·m^{-2}), and more absorbing particles (decrease in the SSA of 0.03) lead to more ARE at the BOA and less at the TOA (4 and 2 W·m^{-2} in absolute terms, respectively). Therefore, the differences among the datasets are within the estimated uncertainty.

The ARE_{SW} values obtained at the BOA and TOA for the three datasets and the averaged value, as well as the FE, are included in

Table 6. Both at the BOA and TOA, the ARE_{SW} has a cooling effect, as expected for mineral dust in this region according to values obtained in the literature (e.g. Sicard et al. 2014a, Mallet et al., 2016). Differences among the three datasets lead to variations in the ARE_{SW} of up to a 30% (or a 20% for the FE), observing larger variability on June 16. The values of the ARE_{SW} and the FE_{SW} are highly dependent on the SZA and a straightforward comparison with previous studies is not simple. Nonetheless, the values obtained for this case are within the range of previous values observed in the western Mediterranean region for similar values of SZA, e.g. FE between -263.4 and -157.1 $W \cdot m^{-2}$ at the BOA and -23.8 and -86.2 $W \cdot m^{-2}$ for SZA=60° or ARE values ranging between -93.1 to -0.5 $W \cdot m^{-2}$ at the BOA and -34.5 to +8.5 $W \cdot m^{-2}$ at the TOA for different SZA values (e.g. Gomez-Amo et al., 2011; Sicard et al., 2014a,b; Barragan et al., 2017).

[Table 6]

[Figure 8]

4.2. LW radiative fluxes

Figure 9 shows F_{LW} calculated with GAME after obtaining the aerosol properties in the LW spectral range from Mie calculations for the three mentioned datasets (see Section 3.2.2). F_{LW} measured by pyrgeometers located onboard the ATR is also shown.

In general, differences in the F_{LW} are always lower than 6% (lower than 10 $W \cdot m^{-2}$ on average), with the airborne values being overestimated by the model on 16 June and underestimated on 17 June. On this latter day, larger differences are observed on the Net F_{LW} compared to 16 June, which might be explained by the inaccurate value of LST used due to the lack of precise data. A sensitivity test performed by increasing the air surface temperature measured at the meteorological station 5K indicates that the $^{\uparrow}F_{LW}$ increases its value up to 30 $W \cdot m^{-2}$ at the surface, and around 10 $W \cdot m^{-2}$ from 1 km onwards which is non-negligible. This would lead to an overestimation of the aircraft measured values, but still within a 6% difference. This highlights the need for accurate LST measurements for radiation simulations in the LW spectral range. Additionally, a sensitivity test performed by assuming a 10% uncertainty in the PSD parameters (r_{eff}, N and σ) leads to an estimated uncertainty of the F_{LW} retrieved by GAME of around 1.2 $W \cdot m^{-2}$. As stated before, the assumption of the refractive index can also introduce variations as large as 0.8 $W \cdot m^{-2}$. Considering the uncertainty of the pyrgeometer and the fact that the aircraft and the model present different vertical resolutions and time samplings and the uncertainties due to the use of the standard atmosphere or the parameterization of the surface properties, the obtained differences are not significant.

[Figure 9]

A comparison of GAME results against the observations from ground-based pyrgeometer at Granada station is included in Figure 10. At the BOA, the longwave radiation measured by the pyrgeometer is in quite good agreement with GAME calculations on 16 June, with differences within 1 $W \cdot m^{-2}$. However, GAME overestimates the pyrgeometer data by 5 $W \cdot m^{-2}$ (1.3%) on 17 June. These difference on June 17, even though larger than on June 16, is still within the uncertainty limits.

[Figure 10]

As for the ARE_{LW}, Figure 11 shows the profiles obtained with GAME using the three datasets as inputs. Values at the BOA and TOA for each dataset and the average values are included in Table 7, together with the FE. Opposite to the SW, the ARE_{LW} produces a heating effect both at the BOA and TOA, with positive values. The slight differences in the F^{LW} in Figure 9 due to the use of different aerosol input datasets lead to variations of up to 2 $W \cdot m^{-2}$ in the $^{BOA}ARE_{LW}$ (ranging from 20 to 26%), which needs to be considered in the interpretation of the results and reduced for a better estimate of the direct ARE. Despite this, values obtained for this dust event (3.2 $W \cdot m^{-2}$ on average for both days) are in agreement with previous studies performed for mineral dust in the infrared region (Sicard et al., 2014a; 2014b) and the FE obtained are comparable to those reported by Meloni et al., (2018). It is extremely interesting to look at the differences between the two days in terms of AOD (ΔAOD) and the effective radius for the coarse mode, $r_{eff,c}$, ($\Delta r_{eff,c}$) and their implication on the differences in the ARE_{LW} at the BOA ($\Delta^{BOA}ARE_{LW}$). For DS1 ΔAOD ($\Delta r_{eff,c}$) is -0.02 (+0.18 μm) which produces a decrease in $^{BOA}ARE_{LW}$ ($\Delta^{BOA}ARE_{LW}$ = -0.5 $W \cdot m^{-2}$). For DS2, ΔAOD ($\Delta r_{eff,c}$) is -0.04 (+0.18 μm) which produces a decrease in $^{BOA}ARE_{LW}$ ($\Delta^{BOA}ARE_{LW}$ = -1.0 $W \cdot m^{-2}$). If we relate these variations to the sensitivity study of Sicard et al. (2014a), in both cases the expected ARE_{LW} increase due to the increase of the coarse mode radii is counterbalanced by the ARE_{LW} decrease when AOD decreases. Oppositely, for DS3 ΔAOD (Δr_c) is -0.05 (+0.64 μm), producing an increase of $^{BOA}ARE_{LW}$ ($\Delta^{BOA}ARE_{LW}$ = +1.6 $W \cdot m^{-2}$). Here, the large increase of the coarse mode radius dominates over the AOD decrease. Sicard et al. (2014a) show indeed that the largest positive gradient of ARE_{LW} occurs for median radii ranging from 0.1 to 2.0 μm. For DS3 the increase of $^{BOA}ARE_{LW}$ produced by a positive Δr_c is larger than the decrease of $^{BOA}ARE_{LW}$ that would have produced ΔAOD alone. At the TOA, same trends, but much less marked, are observed.

[Figure 11]

[Table 7]

4.3. Total mineral dust radiative effect

The total ARE, including both the SW and LW component, is included in Figure 12 and Table 8. As observed, mineral dust produces a net cooling effect both at the surface and the TOA on both days. Depending on the input dataset used for the aerosol properties, values can change by up to 15 $W \cdot m^{-2}$. On average, the ^{BOA}ARE (^{BOA}FE) values are -23.8 ± 8.4 (-109.5±27.4) and -29.2 ± 4.0 (-164.7±11.5) $W \cdot m^{-2}$, and the ^{TOA}ARE (^{TOA}FE) is equal to -2.6 ± 2.2 (-13.0±12.3) and -7.0 ± 2.1 (-40.3±14.1) $W \cdot m^{-2}$ on 16 and 17 June, respectively. These values of the FE are comparable to those reported in the literature (Di Biagio et al., 2009; Meloni et al., 2015). The total averaged ARE values are 15 and 13% lower than for the SW spectral range, confirming that the LW fraction cannot be neglected. The ARE_{LW} represents approximately 20% of the ARE_{SW} near the surface (except for DS3 on June 16), and reaches up to 50% at higher altitudes where the total ARE is quite low (see 16 June on Figure 12). Overall these ARE_{LW}/ARE_{SW} ratios are in agreement with those found at the BOA in previous studies for the Mediterranean region, which ranged

between 9 and 26% (di Sarra et al. 2011; Perrone and Bergamo 2011; Sicard et al. 2014a; Meloni et al., 2015). As for the TOA, larger ratios are obtained here on June 16, but it is worthy to note that results are not directly comparable to previous studies because of the differences in SZA and the different vertical resolution in GAME for the SW and LW components above 4 km, which may lead to numeric artifacts in the obtained results.

[Figure 12]

[Table 8]

5 Conclusions

A moderate Saharan dust event affecting the western Mediterranean region during the Charmex/ADRIMED campaign on June 2013 was extensively monitored by ground-based and aircraft instrumentation above Granada experimental site. Radiative fluxes and mineral dust ARE both in the solar and infrared spectral ranges are calculated for this event with the RTM GAME. Three different aerosol input datasets, are used by GAME RTM in order to evaluate the impact of different input data in GAME calculations.

For the SW, very low variability with the input aerosol data (less than 1%) is observed for the radiative fluxes. The evaluation of GAME calculated radiative fluxes against the aircraft data reveals differences between the model fluxes and the measurements below 7%, with better agreement at altitudes above the planetary boundary layer. The differences between the retrievals with the three aerosol datasets are quite insignificant, especially taking into account the different approaches followed by the model and the pyranometers. Thus a conclusion on which input dataset provides a better performance is unlikely. The low differences between GAME radiative fluxes retrievals lead to variations in the ARE_{SW} of up to 33%, mostly driven by the differences in the aerosol vertical distribution and load, followed by the SSA.

For the LW, the effect of the aerosol in the radiative properties is lower compared to the SW, but certainly non-negligible and of opposite sign. GAME retrievals using the three aerosol datasets reveal differences in the fluxes lower than 2 $W \cdot m^{-2}$ (less than 1%). The comparison with the pyrgeometer data measured at the ATR reveals however differences around 7%. Considering the low influence of the aerosol in the LW radiative fluxes, the influence of the assumed CO_2, O_3 and the used water vapor profiles and LST are needed to fully explain this discrepancy between the aircraft and the simulated profiles.

The total ARE, including both the SW and LW components, confirms that mineral dust produces a cooling effect both at the surface and the TOA, as already reported in the literature. On average, the ARE_{LW} represents a 20% of the ARE_{SW} at the surface, therefore clearly indicating that global model estimates need to consider the complete spectrum to avoid an overestimation on mineral dust cooling effect.

Additionally, it is necessary to be aware of the effects of using different measurement techniques and processing methodologies when calculating aerosol radiative properties. Even though the differences observed here when using different aerosol datasets are slight, they still exist and a homogenization of the

techniques to feed global models would be beneficial for a better estimate of the ARE and a reduced uncertainty.

Acknowledgements

This work is part of the ChArMEx project supported by CNRS-INSU, ADEME, Météo-France and CEA in the framework of the multidisciplinary program MISTRALS (Mediterranean Integrated Studies aT Regional And Local Scales; http://mistrals-home.org/). Lidar measurements were supported by the ACTRIS (Aerosols, Clouds, and Trace Gases Research Infrastructure Network) Research Infrastructure Project funded by the European Union's Horizon 2020 research and innovation programme under grant agreement n. 654109. The Barcelona team acknowledges the Spanish Ministry of Economy and Competitivity (project TEC2015-63832-P) and EFRD (European Fund for Regional Development); the Department of Economy and Knowledge of the Catalan autonomous government (grant 2014 SGR 583) and the Unidad de Excelencia Maria de Maeztu (project MDM-2016-0600) financed by the Spanish Agencia Estatal de Investigación. The authors also thank the Spanish Ministry of Sciences, Innovation and Universities (ref. CGL2017-90884-REDT). This work was also supported by the Juan de la Cierva-Formación program (grant FJCI-2015-23904). P. Formenti and C. Denjean acknowledge the support of the French National Research Agency (ANR) through the ADRIMED program (contract ANR-11-BS56-0006). Airborne data was obtained using the aircraft managed by SAFIRE, the French facility for airborne research, an infrastructure of the French National Center for Scientific Research (CNRS), Météo-France and the French National Center for Space Studies (CNES). The authors acknowledge the use of GRASP inversion algorithm (www.grasp-open.com). The authors also kindly acknowledge Philippe Dubuisson (Laboratoire d'Optique Atmosphérique, Université de Lille, France) for the use of GAME model and Rosa Delia García Cabrera for her advice during the preparation of this manuscript.

References

Alados-Arboledas, L., Müller, D., Guerrero-Rascado, J. L., Navas-Guzmán, F., Pérez-Ramírez, D. and Olmo, F. J.: Optical and microphysical properties of fresh biomass burning aerosol retrieved by Raman lidar, and star-and sun-photometry, Geophys. Res. Lett., 38(1), n/a-n/a, doi:10.1029/2010GL045999, 2011.

Antón, M., A. Valenzuela, A. Cazorla, J.E. Gil, J. Fernández-Gálvez, H. Lyamani, I. Foyo-Moreno, F.J. Olmo, L. Alados-Arboledas, Global and diffuse shortwave irradiance during a strong desert dust episode at Granada (Spain), Atmospheric Research, 118, 232-239, doi: 10.1016/j.atmosres.2012.07.007, 2012.

Antón, M., A. Valenzuela, D. Mateos, I. Alados, I. Foyo-Moreno, F.J. Olmo, L. Alados-Arboledas, Longwave aerosol radiative effects during an extreme desert dust event in southeastern Spain, Atmospheric Research, 149, 18-23, doi: 10.1016/j.atmosres.2014.05.022, 2014.

Barragan, R., Sicard, M., Totems, J., Léon, J. F., Dulac, F., Mallet, M., Pelon, J., Alados-Arboledas, L., Amodeo, A., Augustin, P., Boselli, A., Bravo-Aranda, J. A., Burlizzi, P., Chazette, P., Comerón, A., D'Amico, G., Dubuisson, P., Granados-Muñoz,

M. J., Leto, G., Guerrero-Rascado, J. L., Madonna, F., Mona, L., Muñoz-Porcar, C., Pappalardo, G., Perrone, M. R., Pont, V., Rocadenbosch, F., Rodriguez-Gomez, A., Scollo, S., Spinelli, N., Titos, G., Wang, X. and Sanchez, R. Z.: Spatio-temporal monitoring by ground-based and air- and space-borne lidars of a moderate Saharan dust event affecting southern Europe in June 2013 in the framework of the ADRIMED/ChArMEx campaign, Air Qual. Atmos. Heal., 10(3), 261–285, doi:10.1007/s11869-016-0447-7, 2017.

Benavent-oltra, J. A., Román, R., Granados-muñoz, M. J., Pérez-, D., Ortiz-amezcua, P., Denjean, C., Lopatin, A., Lyamani, H., Guerrero-rascado, J. L., Fuertes, D., Dubovik, O., Chaikovsky, A., Olmo, F. J., Mallet, M. and Alados-arboledas, L.: Comparative assessment of GRASP algorithm for a dust event over Granada (Spain) during ChArMEx-ADRIMED 2013 campaign ., Atmos. Meas. Tech., (July), 1–29, 2017.

Boucher, O., Randall, D., Artaxo, P., Bretherton, C., Feingold, G., Forster, P., Kerminen, V., Kondo, Y., Liao, H., Lohmann, U., Rasch, P., Satheesh, S., Sherwood, S., Stevens, B., Zhang, X., Qin, D., Plattner, G., Tignor, M., Allen, S., Boschung, J., Nauels, A., Xia, Y., Bex, V., Midgley, P., Boucher, O. and Randall, D.: Clouds and Aerosols, in Climate Change 2013 - The Physical Science Basis, pp. 571–658., 2013.

Bravo-Aranda, J. A., Navas-Guzmán, F., Guerrero-Rascado, J. L., Pérez-Ramírez, D., Granados-Muñoz, M. J. and Alados-Arboledas, L.: Analysis of lidar depolarization calibration procedure and application to the atmospheric aerosol characterization, Int. J. Remote Sens., 34(9–10), 3543–3560, doi:10.1080/01431161.2012.716546, 2013.

Chen, C., Dubovik, O., Henze, D. K., Lapyonak, T., Chin, M., Ducos, F., Litvinov, P., Huang, X., and Li, L.: Retrieval of Desert Dust and Carbonaceous Aerosol Emissions over Africa from POLDER/PARASOL Products Generated by GRASP Algorithm, Atmos. Chem. Phys. Discuss., https://doi.org/10.5194/acp-2018-35, in review, 2018.

Choobari, O. A., Zawar-Reza, P. and Sturman, A.: The global distribution of mineral dust and its impacts on the climate system: A review, Atmos. Res., 138, 152–165, doi:10.1016/j.atmosres.2013.11.007, 2014.

Denjean, C., Cassola, F., Mazzino, A., Triquet, S., Chevaillier, S., Grand, N., Bourrianne, T., Momboisse, G., Sellegri, K., Schwarzenbock, A., Freney, E., Mallet, M. and Formenti, P.: Size distribution and optical properties of mineral dust aerosols transported in the western Mediterranean, Atmos. Chem. Phys., 16(2), 1081–1104, doi:10.5194/acp-16-1081-2016, 2016.

Di Biagio, C., A. di Sarra, D. Meloni, F. Monteleone, S. Piacentino, and D. Sferlazzo, Measurements of Mediterranean aerosol radiative forcing and influence of the single scattering albedo, J. Geophys. Res., 114, D06211, doi:10.1029/2008JD011037, 2009.

Di Biagio, C., Formenti, P., Balkanski, Y., Caponi, L., Cazaunau, M., Pangui, E., Journet, E., Nowak, S., Caquineau, S., Andreae O, M., Kandler, K., Saeed, T., Piketh, S., Seibert, D., Williams, E. and Doussin, J. F. C.: Global scale variability of the mineral dust long-wave refractive index: A new dataset of in situ measurements for climate modeling and remote sensing, Atmos. Chem. Phys., 17(3), 1901–1929, doi:10.5194/acp-17-1901-2017, 2017.

di Sarra, A., Di Biagio, C., Meloni, D., Monteleone, F., Pace, G., Pugnaghi, S. and Sferlazzo, D.: Shortwave and longwave radiative effects of the intense Saharan dust event of 25-26 March 2010 at Lampedusa (Mediterranean Sea), J. Geophys. Res. Atmos., 116(D23), n/a-n/a, doi:10.1029/2011JD016238, 2011.

Dubovik, O. and King, M. D.: A flexible inversion algorithm for retrieval of aerosol optical properties from Sun and sky radiance measurements, J. Geophys. Res. Atmos., 105(D16), 20673–20696, doi:10.1029/2000JD900282, 2000.

Dubovik, O., Holben, B. N., Lapyonok, T., Sinyuk, A., Mishchenko, M. I., Yang, P. and Slutsker, I.: Non-spherical aerosol retrieval method employing light scattering by spheroids, Geophys. Res. Lett., 29(10), 54-1-54–4, doi:10.1029/2001GL014506, 2002.

Dubovik, O., Sinyuk, A., Lapyonok, T., Holben, B. N., Mishchenko, M., Yang, P., Eck, T. F., Volten, H., Muñoz, O., Veihelmann, B., van der Zande, W. J., Leon, J. F., Sorokin, M. and Slutsker, I.: Application of spheroid models to account for aerosol particle nonsphericity in remote sensing of desert dust, J. Geophys. Res. Atmos., 111(11), D11208, doi:10.1029/2005JD006619, 2006.

Dubovik, O., Herman, M., Holdak, A., Lapyonok, T., Tanré, D., Deuzé, J. L., Ducos, F., Sinyuk, A. and Lopatin, A.: Statistically

optimized inversion algorithm for enhanced retrieval of aerosol properties from spectral multi-angle polarimetric satellite observations, Atmos. Meas. Tech., 4(5), 975–1018, doi:10.5194/amt-4-975-2011, 2011.

Dubovik, Oleg, et al. "GRASP: a versatile algorithm for characterizing the atmosphere." SPIE Newsroom 25, 2014.

Dubuisson, P., Buriez, J. C. and Fouquart, Y.: High spectral resolution solar radiative transfer in absorbing and scattering media: Application to the satellite simulation, J. Quant. Spectrosc. Radiat. Transf., 55(1), 103–126, doi:10.1016/0022-4073(95)00134-4, 1996.

Dubuisson, P., Dessailly, D., Vesperini, M. and Frouin, R.: Water vapor retrieval over ocean using near-infrared radiometry, J. Geophys. Res. D Atmos., 109(19), doi:10.1029/2004JD004516, 2004.

Dubuisson, P., Giraud, V., Chomette, O., Chepfer, H. and Pelon, J.: Fast radiative transfer modeling for infrared imaging radiometry, J. Quant. Spectrosc. Radiat. Transf., 95(2), 201–220, doi:10.1016/j.jqsrt.2004.09.034, 2005.

Eck, T. F., Holben, B. N., Reid, J. S., Dubovik, O., Smirnov, A., O'Neill, N. T., Slutsker, I. and Kinne, S.: Wavelength dependence of the optical depth of biomass burning, urban, and desert dust aerosols, J. Geophys. Res. Atmos., 104(D24), 31333–31349, doi:10.1029/1999JD900923, 1999.

Espinosa, W.R., Remer, L.A., Dubovik, O., Ziemba, L., Beyersdorf, A., Orozco, D., Schuster, G., Lapyonok, T., Fuertes, D., Martins, J.V. Retrievals of aerosol optical and microphysical properties from imaging polar nephelometer scattering measurements. Atmos. Meas. Tech. 10, 811–824, 2017.

Fernald, F. G.: Analysis of atmospheric lidar observations:, , 23(5) [online] Available from: https://www.osapublishing.org/DirectPDFAccess/12641A7B-F076-A356-C26E134E8E22E7F2_27314/ao-23-5-652.pdf?da=1&id=27314&seq=0&mobile=no (Accessed 26 April 2018), 1984.

Fernald, F. G., Herman, B. M. and Reagan, J. A.: Determination of Aerosol Height Distributions by Lidar, J. Appl. Meteorol., 11(3), 482–489, doi:10.1175/1520-0450(1972)011<0482:DOAHDB>2.0.CO;2, 1972.

Formenti, P., Schütz, L., Balkanski, Y., Desboeufs, K., Ebert, M., Kandler, K., Petzold, A., Scheuvens, D., Weinbruch, S. and Zhang, D.: Recent progress in understanding physical and chemical properties of African and Asian mineral dust, Atmos. Chem. Phys., 11(16), 8231–8256, doi:10.5194/acp-11-8231-2011, 2011.

Franke, K., Ansmann, A., Müller, D., Althausen, D., Wagner, F. and Scheele, R.: One-year observations of particle lidar ratio over the tropical Indian Ocean with Raman lidar, Geophys. Res. Lett., 28(24), 4559–4562, doi:10.1029/2001GL013671, 2001.

García, O. E., Díaz, A. M., Expósito, F. J., Díaz, J. P., Dubovik, O., Dubuisson, P., Roger, J.-C., Eck, T. F., Sinyuk, A., Derimian, Y., Dutton, E. G., Schafer, J. S., Holben, B. N., and García, C. A.: Validation of AERONET estimates of atmospheric solar fluxes and aerosol radiative forcing by groundbased broadband measurements, J. Geophys. Res., 113, D21207, doi:10.1029/2008JD010211, 2008.

Ginoux, P., Prospero, J. M., Gill, T. E., Hsu, N. C. and Zhao, M.: Global-scale attribution of anthropogenic and natural dust sources and their emission rates based on MODIS Deep Blue aerosol products, Rev. Geophys., 50(3), doi:10.1029/2012RG000388, 2012.

Gkikas, A., Hatzianastassiou, N., Mihalopoulos, N., Katsoulis, V., Kazadzis, S., Pey, J., Querol, X. and Torres, O.: The regime of intense desert dust episodes in the Mediterranean based on contemporary satellite observations and ground measurements, Atmos. Chem. Phys., 13(23), 12135–12154, doi:10.5194/acp-13-12135-2013, 2013.

Gómez-Amo, J.L., A.diSarra, D.Meloni, M.Cacciani, M.P.Utrillas, Sensitivity of shortwave radiative fluxes to the vertical distribution of aerosol single scattering albedo in the presence of a desert dust layer, Atmospheric Environment 44, 2787-2791, 2010.

Gómez-Amo, J.L., V. Pinti, T. Di Iorio, A. di Sarra, D. Meloni, S. Becagli, V. Bellantone, M. Cacciani, D. Fuà, M.R. Perrone, The June 2007 Saharan dust event in the central Mediterranean: Observations and radiative effects in marine, urban, and sub-urban environments, Atmospheric Environment 45, 5385-5393, 2011.

Guan, H., B. Schmid, A. Bucholtz, and R. Bergstrom, Sensitivity of shortwave radiative flux density, forcing, and heating rate

to the aerosol vertical profile, Journal of Geophysical Research, 115, D06209, doi:10.1029/2009JD012907, 2010.

Hess, M., Koepke, P. and Schult, I.: Optical Properties of Aerosols and Clouds: The Software Package OPAC, Bull. Am. Meteorol. Soc., 79(5), 831–844, doi:10.1175/1520-0477(1998)079<0831:OPOAAC>2.0.CO;2, 1998.

Holben, B. N., Eck, T. F., Slutsker, I., Tanré, D., Buis, J. P., Setzer, A., Vermote, E., Reagan, J. A., Kaufman, Y. J., Nakajima, T., Lavenu, F., Jankowiak, I. and Smirnov, A.: AERONET - A federated instrument network and data archive for aerosol characterization, Remote Sens. Environ., 66(1), 1–16, doi:10.1016/S0034-4257(98)00031-5, 1998.

Israelevich, P., Ganor, E., Alpert, P., Kishcha, P. and Stupp, A.: Predominant transport paths of Saharan dust over the Mediterranean Sea to Europe, J. Geophys. Res. Atmos., 117(2), n/a-n/a, doi:10.1029/2011JD016482, 2012.

Karol, Y., Tanré, D., Goloub, P., Vervaerde, C., Balois, J. Y., Blarel, L., Podvin, T., Mortier, A. and Chaikovsky, A.: Airborne sun photometer PLASMA: Concept, measurements, comparison of aerosol extinction vertical profile with lidar, Atmos. Meas. Tech., 6(9), 2383–2389, doi:10.5194/amt-6-2383-2013, 2013.

Klett, J. D.: Stable analytical inversion solution for processing lidar returns, Appl. Opt., 20(2), 211, doi:10.1364/AO.20.000211, 1981.

Klett, J. D.: Lidar inversion with variable backscatter/extinction ratios, Appl. Opt., 24(11), 1638, doi:10.1364/AO.24.001638, 1985.

Kokhanovsky, A.A., Davis, A.B., Cairns, B., Dubovik, O., Hasekamp, O.P., Sano, I., Mukai, S., Rozanov, V.V., Litvinov, P., Lapyonok, T., Kolomiets, I.S., Oberemok, Y.A., Savenkov, S., Martin, W., Wasilewski, A., Di Noia, A., Stap, F.A., Rietjens, J., Xu, F., Natraj, V., Duan, M., Cheng, T., Munro, R. Space-based remote sensing of atmospheric aerosols: the multi-angle spectro-polarimetric frontier. Earth Sci. Rev. 145, 85–116, 2015.

Krekov, G. M.: Models of atmospheric aerosols. In: Jennings SG (ed), Aerosol effects on climate. University of Arizona Press, Tucson, AZ, pp. 9–72, 1993.

Landulfo, E., Papayannis, A., Artaxo, P., Castanho, A. D. A., De Freitas, A. Z., Souza, R. F., Vieira, N. D., Jorge, M. P. M. P., Sánchez-Ccoyllo, O. R. and Moreira, D. S.: Synergetic measurements of aerosols over São Paulo, Brazil using LIDAR, sunphotometer and satellite data during the dry season, Atmos. Chem. Phys., 3(5), 1523–1539, doi:10.5194/acp-3-1523-2003, 2003.

Levy, R. C., Mattoo, S., Munchak, L. A., Remer, L. A., Sayer, A. M., Patadia, F. and Hsu, N. C.: The Collection 6 MODIS aerosol products over land and ocean, Atmos. Meas. Tech., 6(11), 2989–3034, doi:10.5194/amt-6-2989-2013, 2013.

Lolli, S., Madonna, F., Rosoldi, M., Campbell, J. R., Welton, E. J. and Lewis, J. R.: Impact of varying lidar measurement and data processing techniques in evaluating cirrus cloud and aerosol direct radiative effects, Atmos. Meas. Tech., 11, 1639–1651, 2018.

Lopatin, A., Dubovik, O., Chaikovsky, A., Goloub, P., Lapyonok, T., Tanré, D. and Litvinov, P.: Enhancement of aerosol characterization using synergy of lidar and sun-photometer coincident observations: The GARRLiC algorithm, Atmos. Meas. Tech., 6(8), 2065–2088, doi:10.5194/amt-6-2065-2013, 2013.

Lyamani, H., Olmo, F. J. and Alados-Arboledas, L.: Saharan dust outbreak over southeastern Spain as detected by sun photometer, Atmos. Environ., 39(38), 7276–7284, doi:10.1016/j.atmosenv.2005.09.011, 2005.

Mallet, M., Pont, V., Liousse, C., Gomes, L., Pelon, J., Osborne, S., Haywood, J., Roger, J., Dubuisson, P., Mariscal, A., Thouret, V., and Goloub, P.: Aerosol direct radiative forcing over Djougou (northern Benin) during the African Monsoon Multidisciplinary Analysis dry season experiment (Special Observation Period-0), J. Geophys. Res. 113, D00C01, doi:10.1029/2007JD009419, 2008.

Mallet, M., Dulac, F., Formenti, P., Nabat, P., Sciare, J., Roberts, G., Pelon, J., Ancellet, G., Tanré, D., Parol, F., Denjean, C., Brogniez, G., di Sarra, A., Alados-Arboledas, L., Arndt, J., Auriol, F., Blarel, L., Bourrianne, T., Chazette, P., Chevaillier, S., Claeys, M., D'Anna, B., Derimian, Y., Desboeufs, K., Di Iorio, T., Doussin, J.-F., Durand, P., Féron, A., Freney, E., Gaimoz, C., Goloub, P., Gómez-Amo, J. L., Granados-Muñoz, M. J., Grand, N., Hamonou, E., Jankowiak, I., Jeannot, M., Léon, J.-F., Maillé, M., Mailler, S., Meloni, D., Menut, L., Momboisse, G., Nicolas, J., Podvin, T., Pont, V., Rea, G., Renard,

J.-B., Roblou, L., Schepanski, K., Schwarzenboeck, A., Sellegri, K., Sicard, M., Solmon, F., Somot, S., Torres, B., Totems, J., Triquet, S., Verdier, N., Verwaerde, C., Waquet, F., Wenger, J., and Zapf, P.: Overview of the Chemistry-Aerosol Mediterranean Experiment/Aerosol Direct Radiative Forcing on the Mediterranean Climate (ChArMEx/ADRIMED) summer 2013 campaign, Atmos. Chem. Phys., 16, 455-504, doi:10.5194/acp-16-455-2016, 2016.

Markowicz, K. M., Flatau, P. J., Vogelmann, A. M., Quinn, P. K. and Welton, E. J.: Clear-sky infrared aerosol radiative forcing at the surface and the top of the atmosphere, Q. J. R. Meteorol. Soc., 129(594 PART A), 2927–2947, doi:10.1256/003590003769682110, 2003.

Meloni, D., Junkermann, W., di Sarra, A., Cacciani, M., De Silvestri, L., Di Iorio, T., Estellés, V., Gómez-Amo, J. L., Pace, G. and Sferlazzo, D. M.: Altitude-resolved shortwave and longwave radiative effects of desert dust in the Mediterranean during the GAMARF campaign: Indications of a net daily cooling in the dust layer, J. Geophys. Res., 120(8), 3386–3407, doi:10.1002/2014JD022312, 2015.

Meloni, D., Di Sarra, A., Brogniez, G., Denjean, C., De Silvestri, L., Di Iorio, T., Formenti, P., Gómez-Amo, J. L., Gröbner, J., Kouremeti, N., Liuzzi, G., Mallet, M., Pace, G. and Sferlazzo, D. M.: Determining the infrared radiative effects of Saharan dust: A radiative transfer modelling study based on vertically resolved measurements at Lampedusa, Atmos. Chem. Phys., 18(6), 4377–4401, doi:10.5194/acp-18-4377-2018, 2018.

Moulin, C., Lambert, C.E., Dayan, U., Masson, V, Ramonet, M., Bousquet, P., Legrand, M., Balkanski, Y. J., Guelle, W., Marticorena, B., Bergametti, G., and Dulac, F.: Satellite climatology of African dust transport in the Mediterranean atmosphere, J. Geophys. Res., 103, 13137-13144, doi:10.1029/98JD00171, 1998.

Nabat, P., Somot, S., Mallet, M., Michou, M., Sevault, F., Driouech, F., Meloni, D., di Sarra, A., Di Biagio, C., Formenti, P., Sicard, M., Léon, J.-F., and Bouin, M.-N.: Dust aerosol radiative effects during summer 2012 simulated with a coupled regional aerosol–atmosphere–ocean model over the Mediterranean, Atmos. Chem. Phys., 15, 3303-3326, doi:10.5194/acp-15-3303-2015, 2015

Navas-Guzmán, F., Rascado, J. L. G. and Arboledas, L. A.: Retrieval of the lidar overlap function using Raman signals, Opt. Pura Apl, 44(1), 71–75, 2011.

Navas-Guzmán, F., Fernández-Gálvez, J., Granados-Muñoz, M. J., Guerrero-Rascado, J. L., Bravo-Aranda, J. A. and Alados-Arboledas, L.: Tropospheric water vapour and relative humidity profiles from lidar and microwave radiometry, Atmos. Meas. Tech., 7(5), 1201–1211, doi:10.5194/amt-7-1201-2014, 2014.

Ortiz-Amezcua, P., Luis Guerrero-Rascado, J., Granados-Munõz, M. J., Benavent-Oltra, J. A., Böckmann, C., Samaras, S., Stachlewska, I. S., Janicka, L., Baars, H., Bohlmann, S. and Alados-Arboledas, L.: Microphysical characterization of long-range transported biomass burning particles from North America at three EARLINET stations, Atmos. Chem. Phys., 17(9), 5931–5946, doi:10.5194/acp-17-5931-2017, 2017.

Otto, S., De Reus, M., Trautmann, T., Thomas, A., Wendisch, M. and Borrmann, S.: Atmospheric radiative effects of an in situ measured Saharan dust plume and the role of large particles, Atmos. Chem. Phys., 7(18), 4887–4903, doi:10.5194/acp-7-4887-2007, 2007.

Papadimas, C. D., Hatzianastassiou, N., Matsoukas, C., Kanakidou, M., Mihalopoulos, N. and Vardavas, I.: The direct effect of aerosols on solar radiation over the broader Mediterranean basin, Atmos. Chem. Phys., 12(15), 7165–7185, doi:10.5194/acp-12-7165-2012, 2012.

Pappalardo, G., Amodeo, A., Apituley, A., Comeron, A., Freudenthaler, V., Linné, H., Ansmann, A., Bösenberg, J., D'Amico, G., Mattis, I., Mona, L., Wandinger, U., Amiridis, V., Alados-Arboledas, L., Nicolae, D., and Wiegner, M.: EARLINET: towards an advanced sustainable European aerosol lidar network, Atmos. Meas. Tech., 7, 2389–2409, doi:10.5194/amt-7-389-2014, 2014.

Pérez-Ramírez, D., Lyamani, H., Smirnov, A., O´Neill, N. T., Veselovskii, I., Whiteman, D. N., Olmo, F. J. and Alados-Arboledas, L.: Statistical study of day and night hourly patterns of columnar aerosol properties using sun and star photometry, in spiedigitallibrary.org, p. 100010K., 2016.

Peris-Ferrús, C., J.L. Gomez-Amo, C. Marcos, M.D. Freile-Aranda, M.P. Utrillas, J.A. Martínez-Lozano, Heating rate profiles and radiative forcing due to a dust storm in the Western Mediterranean using satellite observations, Atmospheric Environment 160, 142-153, 2017.

Perrone, M. R. and Bergamo, A.: Direct radiative forcing during Sahara dust intrusions at a site in the Central Mediterranean: Anthropogenic particle contribution, Atmos. Res., 101(3), 783–798, doi:10.1016/j.atmosres.2011.05.011, 2011.

Perrone, M. R., Tafuro, A. M. and Kinne, S.: Dust layer effects on the atmospheric radiative budget and heating rate profiles, Atmos. Environ., 59, 344–354, doi:10.1016/J.ATMOSENV.2012.06.012, 2012.

Renard, J.-B., Dulac, F., Durand, P., Bourgeois, Q., Denjean, C., Vignelles, D., Couté, B., Jeannot, M., Verdier, N., and Mallet, M.: In situ measurements of desert dust particles above the western Mediterranean Sea with the balloon-borne Light Optical Aerosol Counter/sizer (LOAC) during the ChArMEx campaign of summer 2013, Atmos. Chem. Phys., 18, 3677-3699, https://doi.org/10.5194/acp-18-3677-2018, 2018.

Roger, J., Mallet, M., Dubuisson, P., Cachier, H., Vermote, E.,Dubovik, O., and Despiau, S.: A synergetic approach for estimating the local direct aerosol forcing: Application to an urban zone during the Expérience sur Site pour Contraindre les Modeles de Pollution et de Transport d'Emission (ESCOMPTE) experiment, J. Geophys. Res. 111, d13208, doi:10.1029/2005JD006361, 2006.

Román, R., Torres, B., Fuertes, D., Cachorro, V.E., Dubovik, O., Toledano, C., Cazorla, A., Barreto, A., Bosch, J.L., Lapyonok, T., González, R., Goloub, P., Perrone, M.R., Olmo, F.J. and Alados-Arboledas, L.: Remote sensing of lunar aureole with a sky camera: Adding infomration in the nocturnal retreival of aerosol properties with GRASP code, Remote Sens. Environ., 196, 238-252, http://dx.doi.org/10.1016/j.rse.2017.05.013, 2017.

Román, R., Benavent-Oltra, J.A., Casquero-Vera, J.A., Lopatin, A., Cazorla, A., Lyamani, H., Denjean, C., Fuertes, D., Pérez-Ramírez, D., Torres, B., Toledano, C., Dubovik, O., Cachorro, V.E., de Frutos, A.M., Olmo, F.J. and Alados-Arboledas, L.: Retrieval of aerosol profiles combining sunphotometer and ceilometer measurements in GRASP code, Atmos. Res., 204, 161-177, https://doi.org/10.1016/j.atmosres.2018.01.021, 2018.

Saunders, R. W., Brogniez, G., Buriez, J. C., Meerkotter, R. and Wendling, P.: A comparison of measured and modeled broadband fluxes from aircraft data during the ICE '89 field experiment, J. Atmos. \& Ocean. Technol., 9(4), 391–406, doi:10.1175/1520-0426(1992)009<0391:ACOMAM>2.0.CO;2, 1992.

Shao, Y., Wyrwoll, K. H., Chappell, A., Huang, J., Lin, Z., McTainsh, G. H., Mikami, M., Tanaka, T. Y., Wang, X. and Yoon, S.: Dust cycle: An emerging core theme in Earth system science, Aeolian Res., 2(4), 181–204, doi:10.1016/j.aeolia.2011.02.001, 2011.

Sicard, M., Mallet, M., García-Vizcaíno, D., Comerón, A., Rocadenbosch, F., Dubuisson, P., and Muñoz-Porcar, C.: Intense dust and extremelly fresh biomass burning in Barcelona, Spain: characterization of their optical properties and estimation of their radiative forcing, Environ. Res. Lett., 7, 034016, doi:10.1088/1748-9326/7/3/034016, 2012.

Sicard, M., Bertolín, S., Mallet, M., Dubuisson, P. and Comerón, A.: Estimation of mineral dust long-wave radiative forcing: Sensitivity study to particle properties and application to real cases in the region of Barcelona, Atmos. Chem. Phys., 14(17), 9213–9231, doi:10.5194/acp-14-9213-2014, 2014a.

Sicard, M., Bertolín, S., Muñoz, C., Rodríguez, A., Rocadenbosch, F. and Comerõn, A.: Separation of aerosol fine- and coarse-mode radiative properties: Effect on the mineral dust longwave, direct radiative forcing, Geophys. Res. Lett., 41(19), 6978–6985, doi:10.1002/2014GL060946, 2014b.

Sicard, M., Barragan, R., Dulac, F., Alados-Arboledas, L. and Mallet, M.: Aerosol optical, microphysical and radiative properties at regional background insular sites in the western Mediterranean, Atmos. Chem. Phys., 16(18), 12177–12203, doi:10.5194/acp-16-12177-2016, 2016.

Stamnes, K., Tsay, S.-C., Wiscombe, W. and Jayaweera, K.: Numerically stable algorithm for discrete-ordinate-method radiative transfer in multiple scattering and emitting layered media, Appl. Opt., 27(12), 2502, doi:10.1364/AO.27.002502, 1988.

Titos, G., del Águila, A., Cazorla, A., Lyamani, H., Casquero-Vera, J. A., Colombi, C., Cuccia, E., Gianelle, V., Močnik, G.,

Alastuey, A., Olmo, F. J. and Alados-Arboledas, L.: Spatial and temporal variability of carbonaceous aerosols: Assessing the impact of biomass burning in the urban environment, Sci. Total Environ., 578, 613–625, doi:10.1016/j.scitotenv.2016.11.007, 2016.

Torres, B., Dubovik, O., Fuertes, D., Schuster, G., Cachorro, V. E., Lapyonok, T., Goloub, P., Blarel, L., Barreto, A., Mallet, M., Toledano, C., and Tanré, D.: Advanced characterisation of aerosol size properties from measurements of spectral optical depth using the GRASP algorithm, Atmos. Meas. Tech., 10, 3743-3781, https://doi.org/10.5194/amt-10-3743-2017, 2017.

Valenzuela, A., Olmo, F. J., Lyamani, H., Antón, M., Quirantes, A. and Alados-Arboledas, L.: Aerosol radiative forcing during African desert dust events (2005-2010) over Southeastern Spain, Atmos. Chem. Phys., 12(21), 10331–10351, doi:10.5194/acp-12-10331-2012, 2012.

Vogelmann, A. M., Flatau, P. J., Szczodrak, M., Markowicz, K. M. and Minnett, P. J.: Observations of large aerosol infrared forcing at the surface, Geophys. Res. Lett., 30(12), doi:10.1029/2002GL016829, 2003.

Wan, Z.: New refinements and validation of the collection-6 MODIS land-surface temperature/emissivity product, Remote Sens. Environ., 140, 36–45, doi:10.1016/j.rse.2013.08.027, 2014.

Yang, P., Feng, Q., Hong, G., Kattawar, G. W., Wiscombe, W. J., Mishchenko, M. I., Dubovik, O., Laszlo, I. and Sokolik, I. N.: Modeling of the scattering and radiative properties of nonspherical dust-like aerosols, J. Aerosol Sci., 38(10), 995–1014, doi:10.1016/j.jaerosci.2007.07.001, 2007.

Zender, C. S.: Mineral Dust Entrainment and Deposition (DEAD) model: Description and 1990s dust climatology, J. Geophys. Res., 108(D14), 4416, doi:10.1029/2002JD002775, 2003.

Zender, C. S., Miller, R. L. R. L. and Tegen, I.: Quantifying mineral dust mass budgets:Terminology, constraints, and current estimates, Eos, Trans. Am. Geophys. Union, 85(48), 509, doi:10.1029/2004EO480002, 2004.

Tables and figures:

	SW	LW
Spectral range [µm]	0.297 – 3.100	4.5 - 40
Vertical range [km]	0-20	0-100
Number of levels	18	40
Vertical resolution (Vertical range) [km]	0.005 (0-0.01) 0.01 (0.01,0.05) 0.05 (0.05-0.1) 0.1 (0.1-0.2) 0.2 (0.2-1) 1 (1-2) 2 (2-10) 5 (10-20)	 1 (0-25) 2.5 (25-50) 5 (50-60 20 (80-100)

Table 1. Summary of GAME main properties for the SW and LW spectral ranges. The altitude range corresponding to the different vertical resolution values is indicated between parentheses.

		SW			LW		
Surface	**alb**	AERONET			CERES		
	LST	IISTA-CEAMA			MODIS		
Met. prof.	**P,T,RH**	Aircraft + US std atm.			Aircraft + US std atm.		
Main gases	**Conc.**	US std atm.			US std atm.		
	Abs.	HITRAN			HITRAN		
		DS 1	**DS 2**	**DS 3**	**DS 1**	**DS 2**	**DS 3**
Aerosol parameters	**α_{aer}**	GRASP (z, 7 λ)	Klett (z, 3 λ)	Aircraft (z, 1 λ)	Mie calculation		
	SSA	GRASP (z, 7 λ)	AERONET (col, 4 λ)	Aircraft (col, 1 λ)			
	g	AERONET (col, 4 λ)	AERONET (col, 4 λ)	AERONET (col, 4 λ)			

Table 2. Summary of the data sources used to obtain the input data parameterizations for GAME computations both in the SW and LW spectral ranges, including the surface parameters (albedo, *alb*, and Land-surface temperature, LST), profiles of meteorological variables and main gases and the aerosol parameters. For the aerosol parameters (aerosol extinction, α_{aer}, single scattering albedo, SSA, and asymmetry parameter, g) three different datasets are used (DS1, DS2 and DS3) based on different instrumentation and retrievals. The indications below the sources of the aerosol parameters indicate whether the parameter is column integrated (col) or if it is vertically resolved (z) and the number of wavelengths at which it is given (n λ).

	alb(440nm)	*alb*(675nm)	*alb*(870nm)	*alb*(1020nm)	*alb*(LW)	LST (K)
June 16	0.05	0.15	0.30	0.30	0.016	314.5
June 17	0.05	0.15	0.31	0.31	0.013	298.1

Table 3. Surface albedo, *alb(λ)*, values provided by AERONET for the SW spectral range and by CERES for the LW. Land-surface temperature (LST) on June 16 was obtained from MODIS whereas on June 17 was estimated from the meteorological station at Granada site. These surface parameters are common to all parameterizations.

16 June (SZA=31.49º)							
	N_f (#·μm^{-2})	N_c (#·μm^{-2})	$r_{eff,f}$ (μm)	$r_{eff,c}$ (μm)	σ_f (μm)	σ_c (μm)	AOD (550 nm)
DS1	9.04	0.018	0.12	2.22	0.48	0.73	0.18
DS2	7.53	0.014	0.12	1.90	0.57	0.65	0.23
DS3	-	-	0.11	1.92	0.63	0.66	0.23
17 June (SZA=61.93º)							
	N_f (#·μm^{-2})	N_c (#·μm^{-2})	$r_{eff,f}$ (μm)	$r_{eff,c}$ (μm)	σ_f (μm)	σ_c (μm)	AOD (550 nm)
DS1	9.04	0.014	0.10	2.40	0.45	0.72	0.16
DS2	8.03	0.012	0.11	2.08	0.53	0.68	0.19
DS3	-	-	0.11	2.56	0.64	0.59	0.18

Table 4. Column-integrated number concentration (*N*), effective radii (r_{eff}) and standard deviation (σ) of fine and coarse aerosol modes and AOD at 550 nm for DS1, DS2 and DS3 on 16 and 17 June.

		LW		
		DS1	**DS2**	**DS3**
Mie calculations	**RI**	DB (2017), (col, 601 λ)	DB (2017), (col, 601 λ)	DB (2017), (col, 601 λ)
	r_{eff}	GRASP (col),	AERONET (col)	Aircraft (z)
	σ	GRASP (col)	AERONET (col)	Aircraft (z)
	N	GRASP (z)	AERONET (col)	Aircraft (z)

Table 5. Summary of the data used to obtain $\alpha_{aer}(\lambda,z)$, SSA(λ,z) and g(λ,z) in the LW from Mie calculations, i.e. the refractive index, RI, effective radius, r_{eff}, geometric standard deviation, σ, and number concentration, *N*. Three different datasets are used (DS1, DS2 and DS3) based on different particle size distribution (PSD) data used. The indications below the sources of the aerosol parameters indicate whether the parameter is column integrated (col) or if it is vertically resolved (*z*) and the number of wavelengths at which it is given (*n λ*). DB(2017) stands for Di Biagio et al., (2017).

	June 16		**June 17**	
	$^{BOA}ARE_{SW}$ (FE) [W·m^{-2}]	**$^{TOA}ARE_{SW}$ (FE) [W·m^{-2}]**	**$^{BOA}ARE_{SW}$ (FE) [W·m^{-2}]**	**$^{TOA}ARE_{SW}$ (FE) [W·m^{-2}]**
DS1	-18.1 (-100.6)	-6.3 (-35.0)	-27.1 (-169.4)	-10.3 (-64.4)

DS2	-28.6 (-124.4)	-5.5 (-23.9)	-34.0 (-178.9)	-9.6 (-50.5)
DS3	-34.3 (-149.1)	-1.5 (-6.5)	-35.8 (-198.9)	-6.5 (-36.1)
Avg ± std. dev	-27.0± 8.2 (-124.7±24.3)	-4.4±2.6 (-21.8±14.4)	-32.3±4.6 (-182.4±15.1)	-8.8±2.0 (50.3±14.2)

Table 6. ARE (and FE indicated between parenthesis) at the BOA and the TOA for the SW spectral range obtained with GAME using as inputs DS1, DS2 and DS3 for June 16 and 17, 2013. The averaged values and standard deviation are also included.

	June 16		**June 17**				
	$^{BOA}ARE_{LW}$ (W·m^{-2})	**$^{TOA}ARE_{LW}$ (W·m^{-2})**	**$^{BOA}ARE_{LW}$ (W·m^{-2})**	**$^{TOA}ARE_{LW}$ (W·m^{-2})**	**ΔAOD**	**Δr_c (μm)**	**$\Delta^{BOA}ARE_{LW}$ (W·m^{-2})**
DS1	+3.1 (+17.2)	+2.2 (+12.2)	+2.6 (+16.3)	+1.6 (+10.0)	-0.02	+0.18	-0.5
DS2	+3.9 (+17.0)	+2.9 (+12.6)	+2.9 (+15.3)	+1.7 (+8.9)	-0.04	+0.18	-1.0
DS3	+2.5 (+10.9)	+1.3 (+5.7)	+4.1 (+22.8)	+1.8 (+10.0)	-0.05	+0.64	+1.6
Avg ± std. dev	+3.2±0.7 (+15.0±3.6)	+2.1±0.8 (+10.2±3.9)	+3.2±0.8 (+18.1±4.1)	+1.7±0.1 (+9.6±0.6)			

Table 7. ARE (and FE indicated between parenthesis) at the BOA and the TOA for the LW spectral range obtained with GAME using as inputs DS1, DS2 and DS3 for June 16 and 17, 2013. The averaged values and standard deviation are also included. The last three columns include variations (Δ) of AOD, r_c and ARE at the BOA between June 16 an 17 for the three datasets.

	June 16		**June 17**	
	^{BOA}ARE (W·m^{-2})	**^{TOA}ARE (W·m^{-2})**	**^{BOA}ARE (W·m^{-2})**	**^{TOA}ARE (W·m^{-2})**
DS1	-15.0 (-83.3)	-4.5 (-25.0)	-24.6 (-153.8)	-8.6 (-53.8)
DS2	-24.7 (-107.4)	-3.1 (-13.5)	-31.1 (-163.7)	-7.8 (-41.1)
DS3	-31.71 (-137.9)	-0.1 (-0.4)	-31.8 (-176.7)	-4.6 (-25.6)
Avg ± std. dev	-23.8±8.4 (-109.5±27.4)	-2.6±2.2 (-13.0±12.3)	-29.2±4.0 (-164.7±11.5)	-7.0±2.1 (-40.3±14.1)

Table 8. ARE (and FE indicated between parenthesis) at the BOA and the TOA for the total (SW+LW) spectral range obtained with GAME using as inputs DS1, DS2 and DS3 for June 16 and 17, 2013. The averaged values and standard deviation are also included.

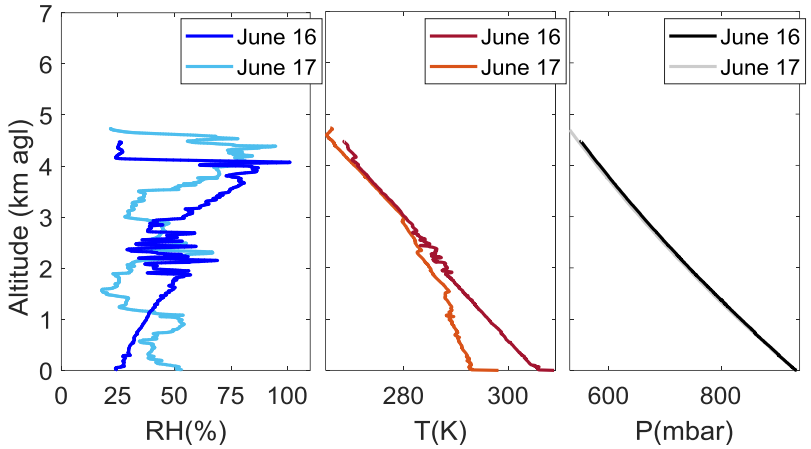

Figure 1. Relative humidity (RH), temperature (T) and pressure (P) profiles measured on-board the ATR during flights F30 (June 16) and F31 (June 17).

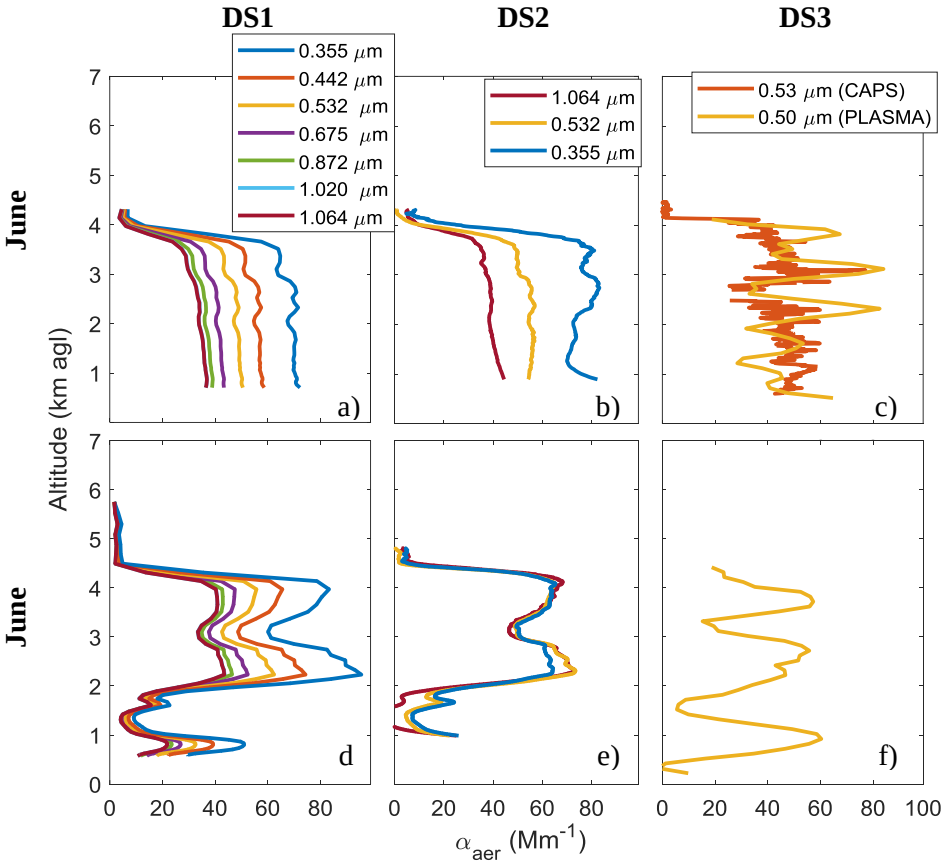

Figure 2. Profiles of α_{aer} obtained from GRASP/DS1 (left), Klett/DS2 (center) and aircraft in-situ/DS3 measurements (right) on June 16 (top row) and June 17 (bottom row).

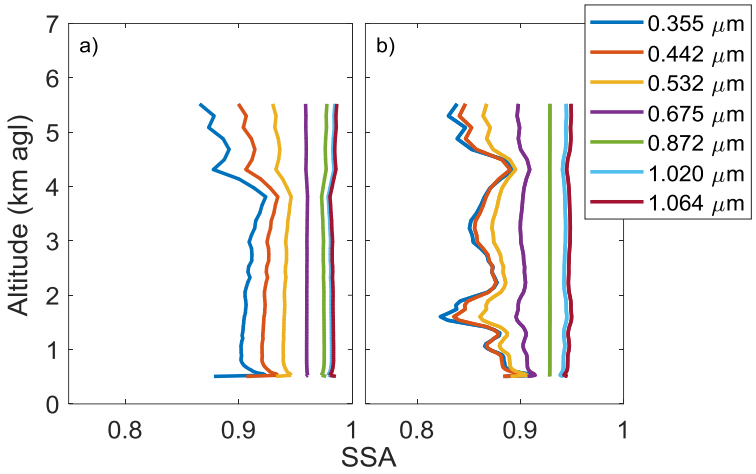

Figure 3. SSA profiles obtained from GRASP/DS1 on June 16 (a) and June 17 (b).

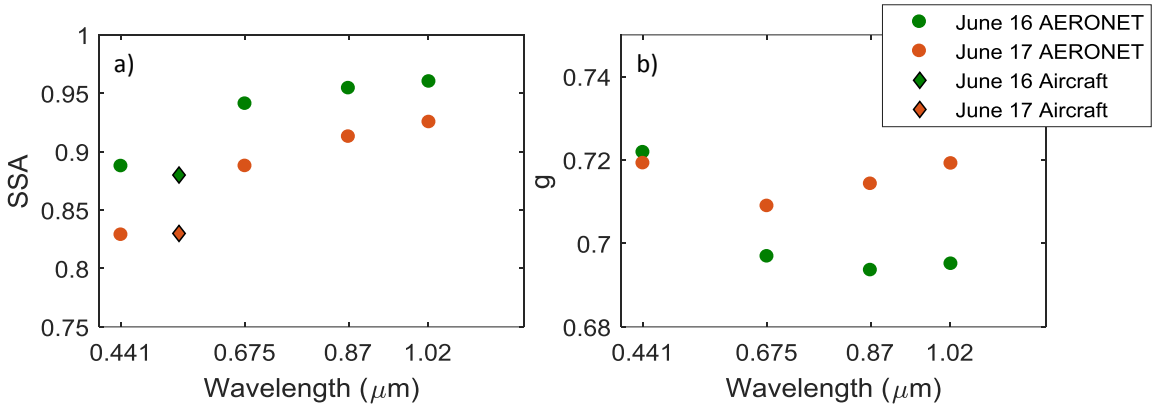

Figure 4. a) AERONET/DS2 column-integrated (circles) and aircraft/DS3 averaged (diamonds) SSA values on June 16 at 16:22UTC and June 17 at 07:20UTC. b) AERONET g values for the same periods.

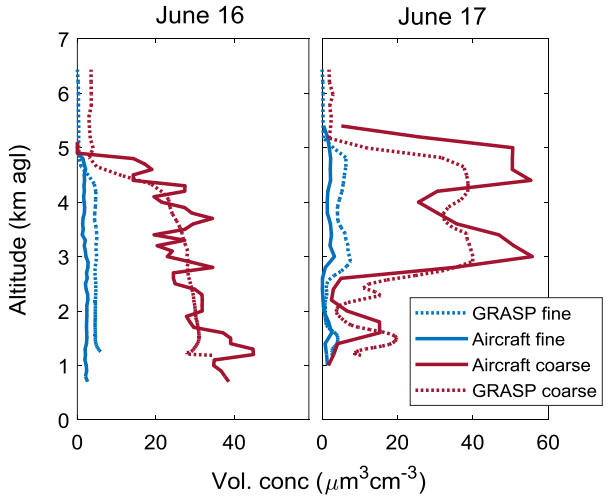

Figure 5. Profiles of aerosol volume concentration for the fine (blue) and coarse (red) mode obtained from GRASP/DS1 (dotted line), and aircraft in-situ/DS3 measurements (solid line) on June 16 (left) and June 17 (right).

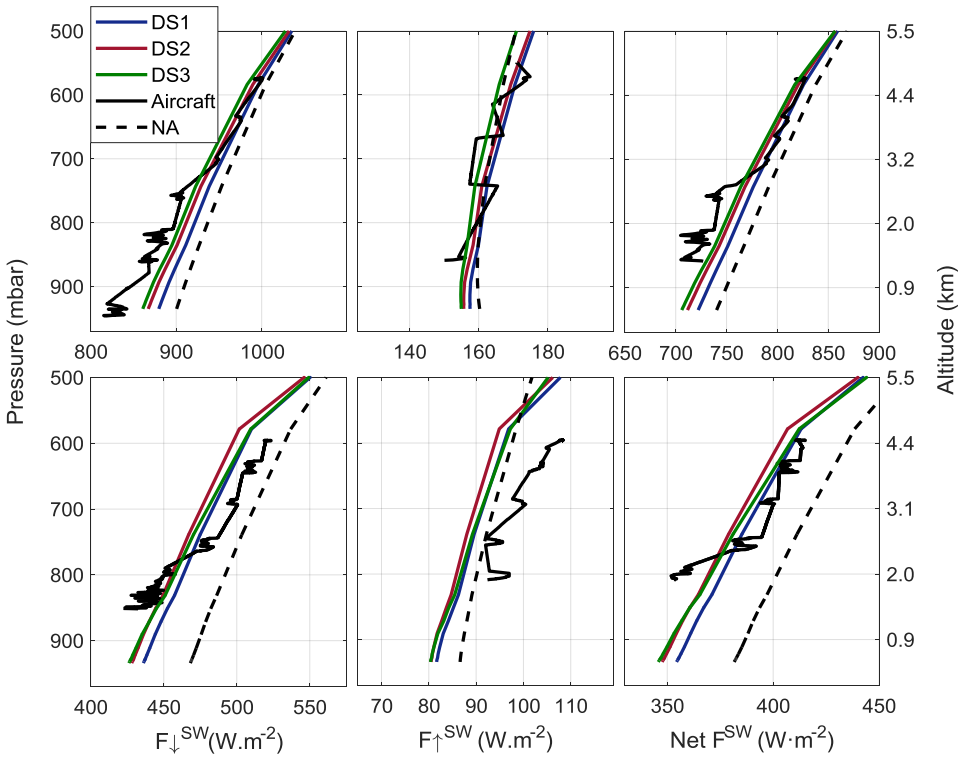

Figure 6. Radiative fluxes for the SW spectral range for June 16 (upper row) and 17 (bottom row) simulated with GAME using different input aerosol datasets (DS1 in blue, DS2 in red and DS3 in green). The black lines are the aircraft in situ measurements distant from about 20 km. The black dashed lines represent the radiative fluxes without the aerosol component (NA).

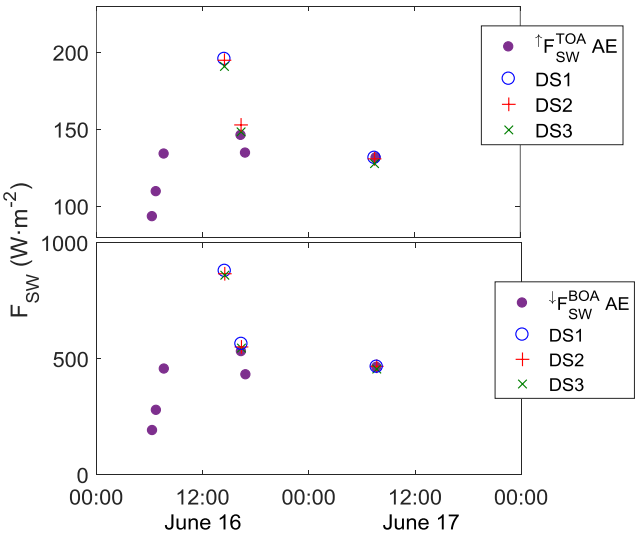

Figure 7. Time series of the $^{\uparrow}F_{SW}$ at the TOA (top) and $^{\downarrow}F_{SW}$ at the BOA (bottom) for the period June 16-17. The purple dots are AERONET fluxes, and GAME ouput data for different inputs are represented by the blue circles (DS1), red (DS2) and green (DS3) crosses.

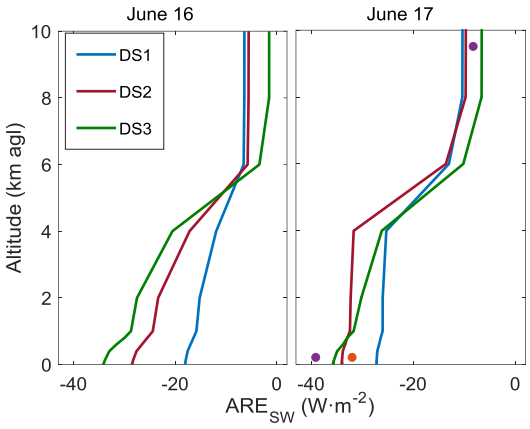

Figure 8. ARE profiles in the SW spectral range simulated using DS1 (blue line), DS2 (red line) and DS3 (green line) as aerosol input data in GAME for June 16 (left) and June 17 (right). The purple dots represent the ARE provided by AERONET (AE) at the BOA and the TOA and the orange dot, the AERONET corrected for the surface albedo effect (AE-C; see text) ARE at the BOA.

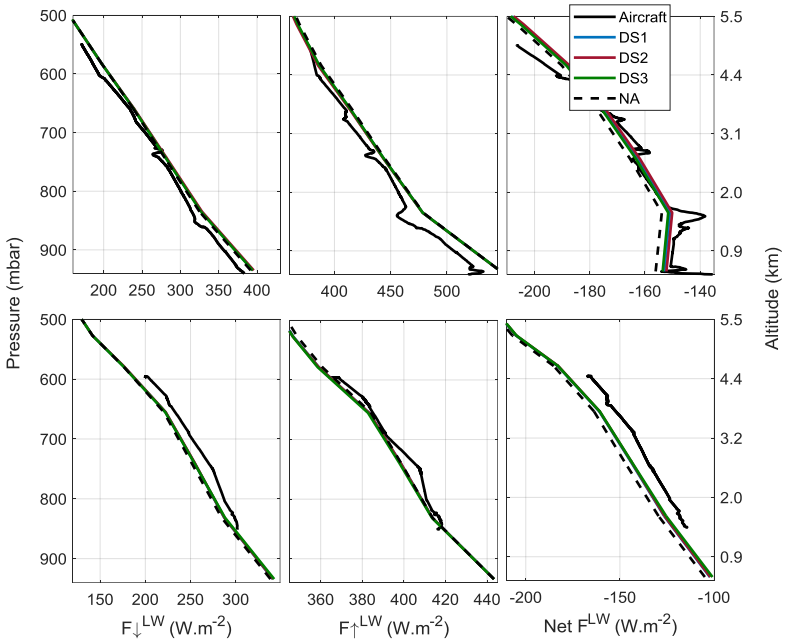

Figure 9. Radiative fluxes for the LW spectral range for June 16 (upper row) and 17 (bottom row) simulated with GAME using different input aerosol datasets (DS1 in blue, DS2 in red and DS3 in green). The black line represents the aircraft in situ measurements. The black dashed lines represent the radiative fluxes without the aerosol component (NA).

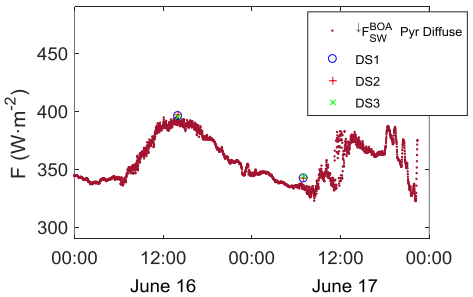

Figure 10. Time series of the $^{\downarrow}F_{LW}$ at the BOA during the period June 16-17. Surface measurements of diffuse (red) radiation from the ground-based pyranometer at Granada station are included. GAME ouput data for different inputs are represented by the blue circles (DS1), red (DS2) and green (DS3) crosses.

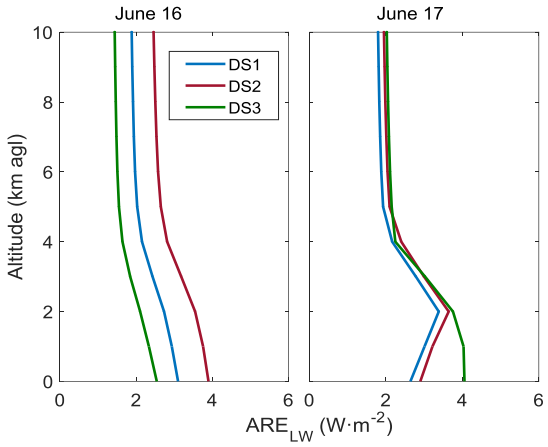

Figure 11. Direct ARE profiles in the LW spectral range simulated using DS1 (blue line), DS2 (red line) and DS3 (green line) as aerosol input data in GAME for June 16 (left) and June 17 (right).

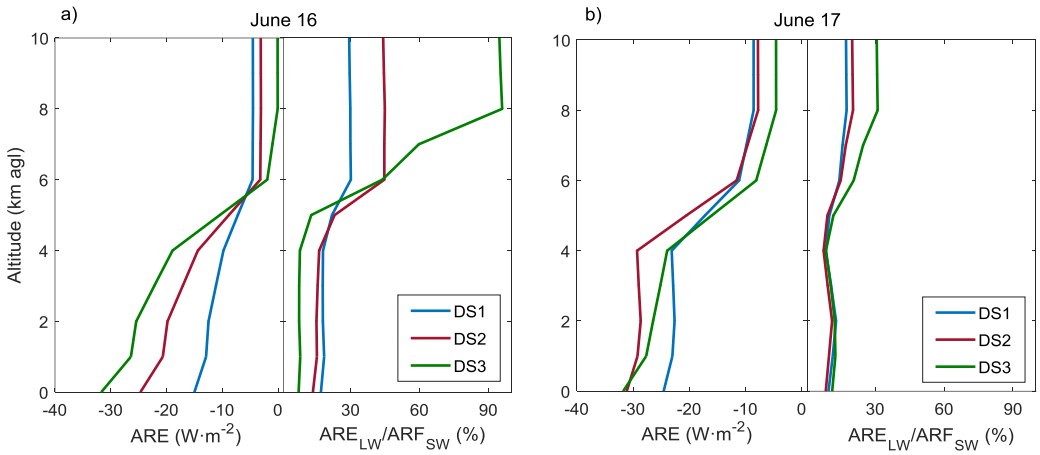

Figure 12. Direct ARE for the total spectrum (left) and the ratio between the ARE LW and the ARE SW in percentage for DS1 (blue), DS2 (red) and DS3 (green) on June 16 at 14:30 UTC (a) and June 17 at 07:30 UTC (b)